

A Data-Driven Model of an Emergency Department, Appendix: Additional Details

Ward Whitt ¹, Xiaopei Zhang ²

Abstract

Armony et al. (2015) carried out an extensive exploratory data analysis of the patient flow through the Rambam Hospital in Israel from a queueing science perspective. In addition, they made a large portion of the data publicly available. We respond by using a portion of that data to analyze the Emergency Department (ED). Our analysis confirms the previous conclusions about the time-varying arrival rate and its consequences, but we also find that the admission probability and the patient length-of-stay distribution should be time varying as well. Our analysis culminates in a new time-varying infinite-server aggregate stochastic model of the ED, where both the length-of-stay distribution and the arrival rate are periodic over a week. Our analysis provides new insights into the arrival, length-of-stay, occupancy and departure processes of this complex system as well as new statistical methods for analyzing ED data.

Keywords: emergency departments, nonstationary stochastic models, queueing models, nonhomogeneous Poisson process, time-varying length-of-stay distribution, two-time-scale arrival process model

1. Introduction

This is an appendix to the main paper [1]. We present additional material that supplements the main paper. This appendix is organized by first having the six sections of the main paper (excluding the conclusions) and then

¹Industrial Engineering and Operations Research, Columbia University, Email: ww2040@columbia.edu, Correspondence to: MailCode 4704, S. W. Mudd Building, 500 West 120th Street, New York NY 10027-6699, U.S.A.

²Industrial Engineering and Operations Research, Columbia University, Email: xz2363@columbia.edu

following by three extra sections covering new material, the first on the time-varying Little’s law [2, 3, 4], which will be expanded upon in [5], the second on fitting birth-and-death processes to the data, which relates to [6, 7, 8], and the third on estimating the extra congestion effect, i.e., how much of the LoS is due to additional waiting caused by congestion as opposed to what can be regarded as the normal required service time. When there is nothing to add to the main paper, as in §2, we leave an empty section.

2. The Rambam Emergency Department and the Data

3. The ED Arrival Process

In this section, we study the arrival process of patients at the ED (by which we always mean the EIMU). In §3.1 we look at the daily totals and then in §3.3 we estimate the hourly arrival rates over a week. We evaluate the stochastic variability in the arrival process in §3.4 which leads to proposing the two-time-scale model involving a conditional nonhomogeneous Poisson process (NHPP). In §3.4.1 we estimate the index of dispersion for counts; in §3.4.2 we report results of statistical tests of the conditional NHPP property, drawing on [9, 10]. In §3.5 we examine the arrival processes of two separate groups of patients: those that are ultimately admitted to one of the IW’s and those that are not. Finally, in §3.6, we summarize the two-time-scale model for the arrival process that we propose, based on that statistical analysis.

3.1. Daily Totals

We first considered a two-factor statistical regression model with Gaussian residuals for the daily total numbers of arrivals; see §§2.7, 3.7 and 6.5 of [11] for background. Here we are only adding to the main paper by showing the histogram of residuals and the Q-Q plot of the Studentized residuals.

To be complete, we repeat the setting. The daily total is represented as

$$T(w, d) \equiv A + Bw + Cd + G(0, \sigma^2), \quad (1)$$

where \equiv denotes equality by definition, w represents the week and d is the day-of-week (DoW), while $G(0, \sigma^2)$ is a mean-0 Gaussian random variable with variance σ^2 (to be estimated) and A , B and C are constants. The week and the DoW are the two factors. Because there is redundancy in model (1), we set $\sum B \equiv 0$ and $\sum C \equiv 0$, so that A gives the average daily total number of arrivals for all days.

Table 1 is the usual Analysis of Variance (ANOVA) table for the regression. From the P -values in the last column of Table 1, we see that both factors

Factor	Sum of square	df	Mean sum of square	F statistics	P-value
Week	10666	24	444.4	2.75	<0.01
DoW	62893	6	10482.2	64.89	<0.01
Residuals	23262	144	161.5		

Table 1: ANOVA table for the two-factor model (1). (Use dataset 3.)

are statistically significant at the 1% level. From the residuals, the estimated variance is $\hat{\sigma}^2 = 161.5 = 12.71^2$. Under this model, the variance-to-mean ratio is $161.5/133.8 = 1.21$. The Gaussian two-factor model is supported by observing that the residuals are consistent with the Gaussian distribution, as can be seen from the histogram of the residuals and the QQ-plot of the studentized residuals in Figure 1. Figure 1(a) is the histogram of the residuals and Figure 1(b) is the QQ-plot of the studentized residuals. The normality assumption looks fairly good. Under this model, the variance-to-mean ratio is $161.5/133.8 = 1.21$.

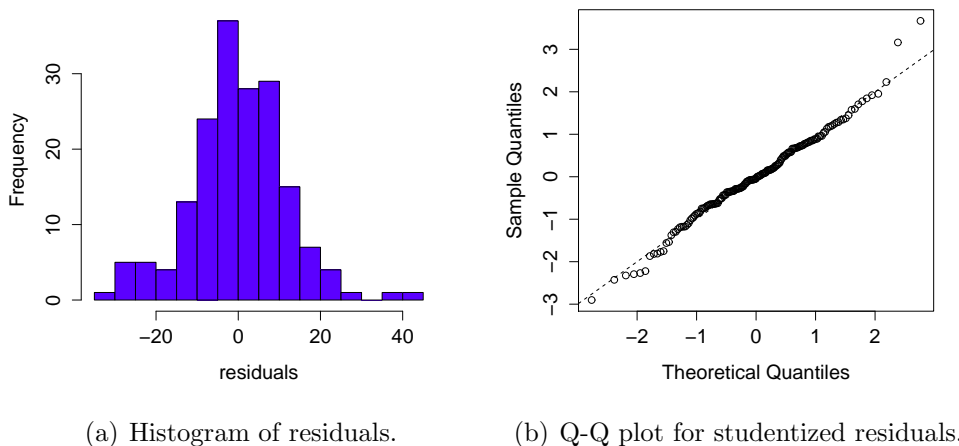


Figure 1: Residuals of regression of daily totals model. (Use data set 3.)

However, our main model for the daily totals is the associated single-factor with only the DoW factor in (2) of the main paper. It is natural to use only the DoW factor because the DoW is known in advance, whereas

the week factor usually is not. The exception might be weeks with Jewish holidays.

3.2. Dependence Among Daily Totals and Residuals

Figure 2 shows a comparison between the actual daily totals (the solid line) and the expected daily totals generated from the single-factor model (the dotted line), while Figure 3 shows a comparison between the actual daily totals (again the solid line) and a realization (sample path) of the daily totals generated from the single-factor model (dotted line). These show reasonable agreement. Figure 4 shows the difference between the data and the predicted values in Figure 2, while Figure 5 does the same for Figure 3. The low week in Figure 1 of the main paper can be seen around day 70.

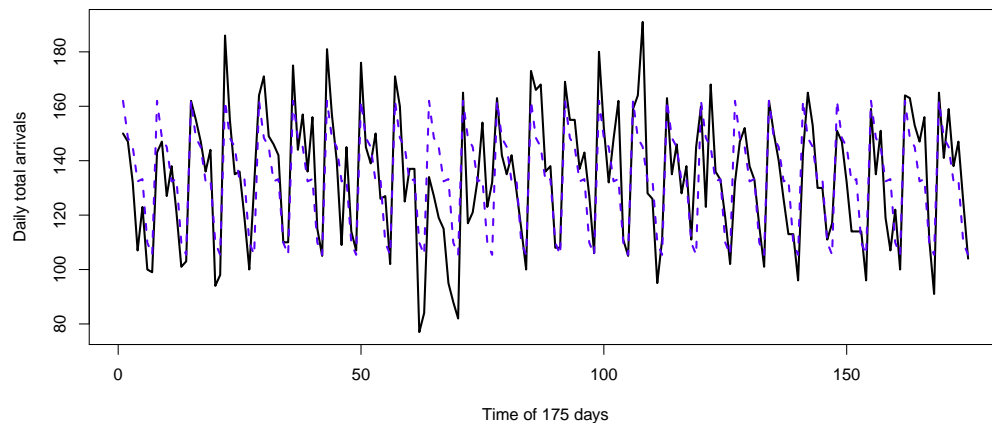


Figure 2: A comparison of the daily totals from the data (solid line) and the Gaussian model mean (Use dataset 3.)

We did four statistical tests of the residuals and found that none could reject the independence hypothesis. Specifically, we performed the Bartles rank test, the difference sign test, the rank test and the turning point test; e.g., see [12]. We also directly estimated the auto-correlation functions (ACF's) for the daily totals and for the residuals. The ACF is defined for a discrete-time process $\{X_t\}, t = 1, 2, \dots, n$ as

$$R(s, t) = \frac{\mathbb{E}((X_t - \mu_t)(X_s - \mu_s))}{\sigma_t \sigma_s},$$

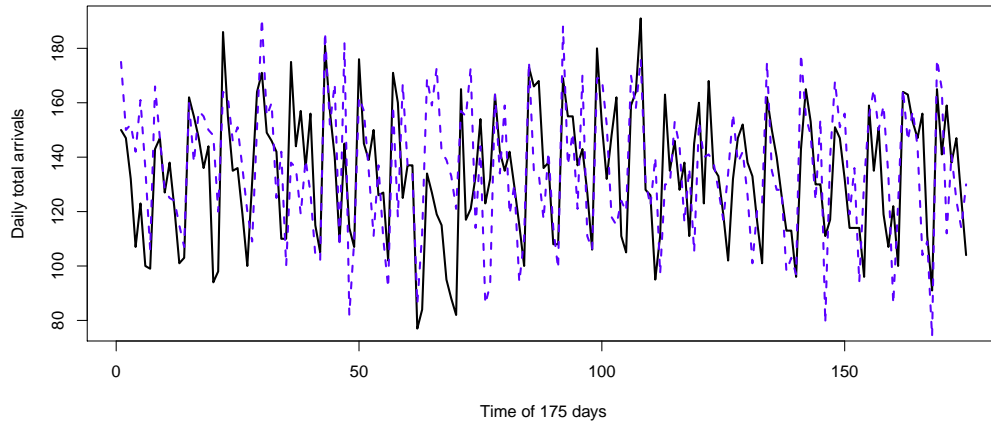


Figure 3: A comparison of the daily totals from the data (solid line) and a realization of the Gaussian model (Use dataset 3.)

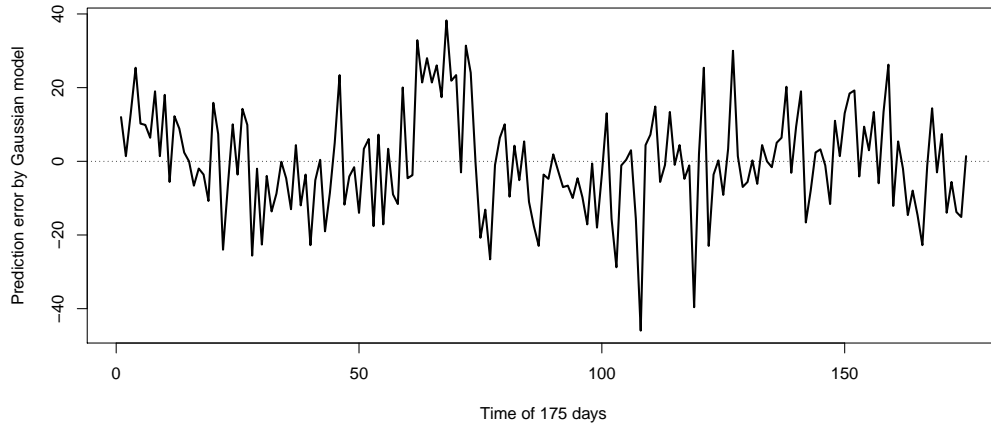


Figure 4: The difference (errors) between the daily totals from the data and the Gaussian model mean (Use dataset 3.)

where μ_t is the expectation of X_t and σ_t is the standard deviation of X_t . If

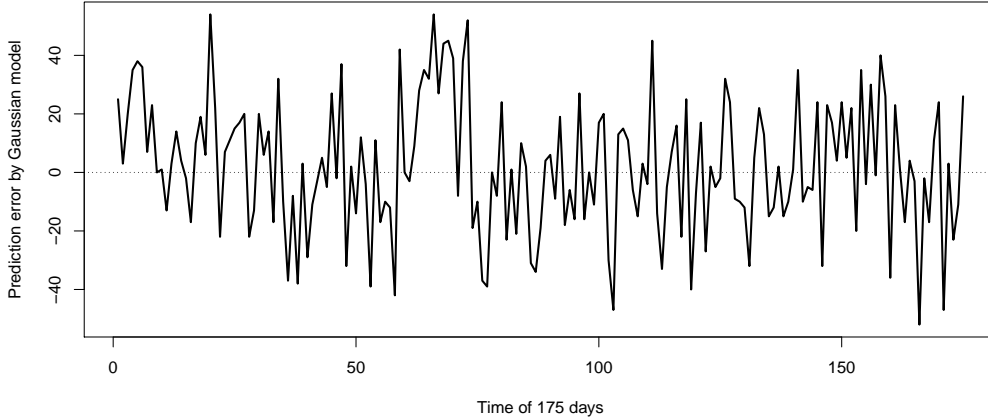


Figure 5: The difference (errors) between the daily totals from the data and a realization of the Gaussian model (Use dataset 3.)

$\{X_t\}$ is stationary, then it can be simplified to

$$R(t) = \frac{\mathbb{E}((X_s - \mu_s)(X_{s+t} - \mu_{s+t}))}{\sigma^2}.$$

Given a sample path of the process, we can estimate the ACF by

$$\hat{R}(t) = \frac{\frac{1}{n-t} \sum_{i=1}^{n-t} ((X_i - \bar{X})(X_{i+t} - \bar{X}))}{\hat{\sigma}^2},$$

where $\bar{X} = \frac{1}{n} \sum_{i=1}^n X_i$ and $\hat{\sigma}^2 = \frac{1}{n-1} \sum_{i=1}^n (X_i - \bar{X})^2$. Figures 6, 7 and 8 shows these ACF's for the daily totals and residuals from the single-factor model by mean prediction and a realization, respectively. The ACF shows positive dependence among the residuals. We refer to [12] for background on the ACF.

We also considered various autoregressive-moving-average time-series models (ARMA(p,q)). An ARMA(p,q) model is of the form

$$X_t = a_0 + \sum_{i=1}^p a_p X_{t-p} + \sum_{i=1}^q b_q \epsilon_{t-q} + \epsilon_t,$$

where a_i, b_i are constants and $\{\epsilon_i\}$ is a sequence of i.i.d. mean-zero Gaussian variables (white noise). We again refer to [12] for more details about

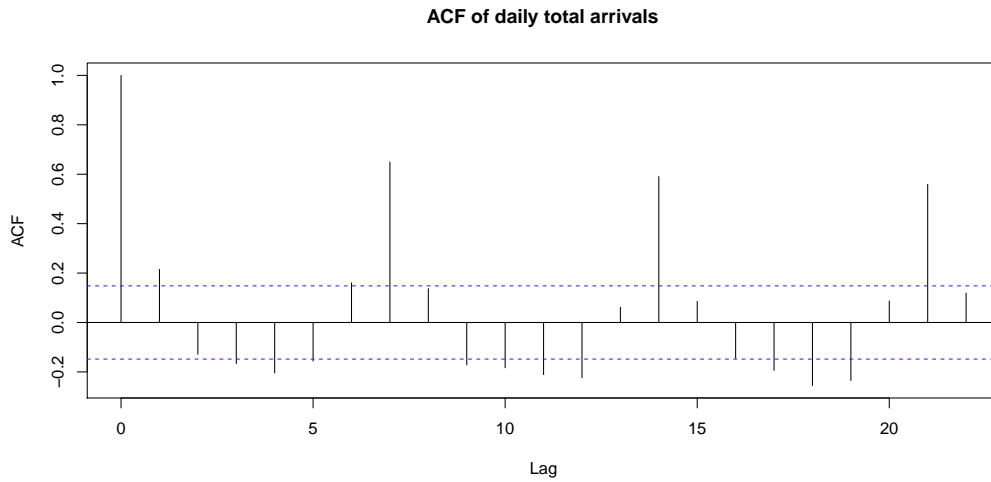


Figure 6: The estimated autocorrelation function for the daily totals (Use dataset 3.)

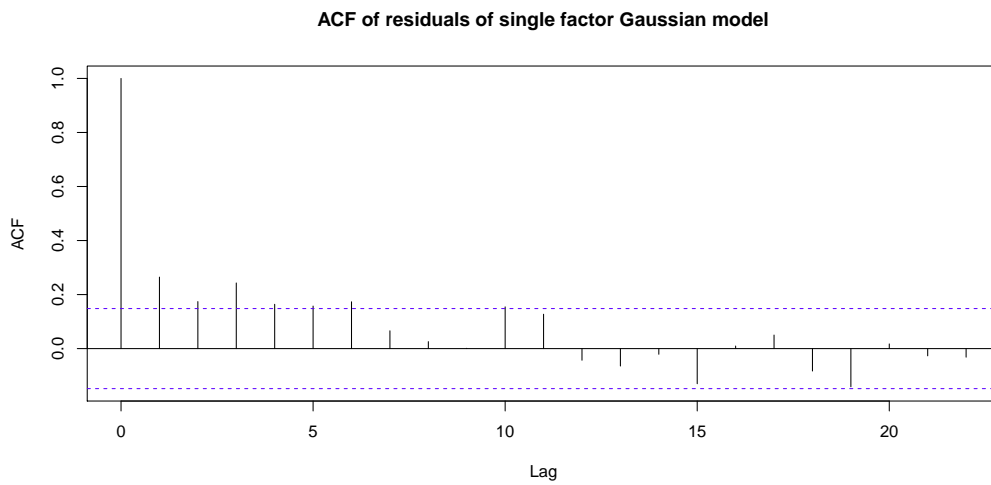


Figure 7: The estimated autocorrelation function for the residuals from the single-factor model by mean prediction (Use dataset 3.)

the ARMA model. We tried $AR(p)$ (which is just $ARMA(p,0)$) models for $1 \leq p \leq 7$ for the residuals, but found that the fitting was not very good. However, the coefficients were almost all positive, indicating that there is some positive dependence among the residuals.

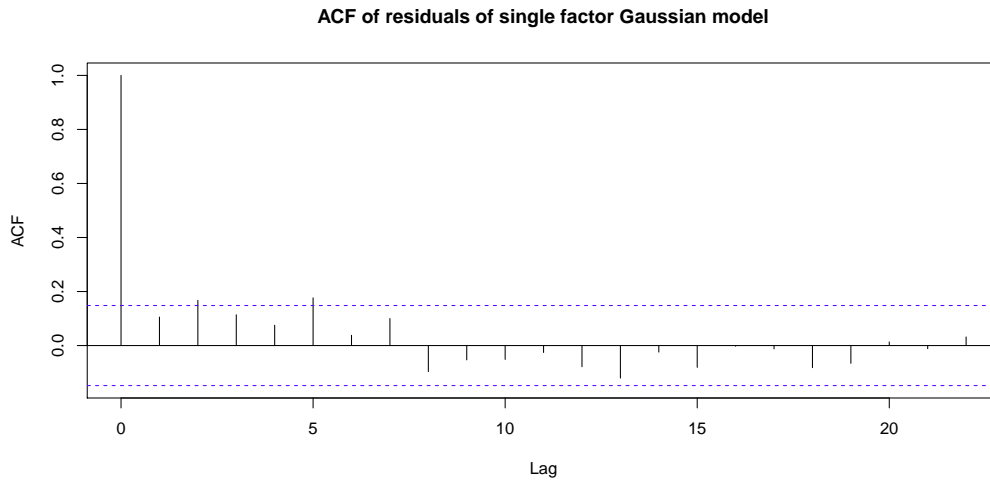


Figure 8: The estimated autocorrelation function for the residuals from the single-factor model by a realization (Use dataset 3.)

We tried $ARMA(p,q)$ models for the true daily totals for various p and q . Based on the established DoW effect, $p = 7$ seems a good choice. The parameter q can capture the long-term effect, but we did not have a large sample. Figure 9 shows a 10-week forecast of the daily totals based on an $ARMA(7,28)$ autoregressive moving average model after the observed 25-week record of daily totals. Figure 10 shows the residuals using the $ARMA(7,28)$ model.

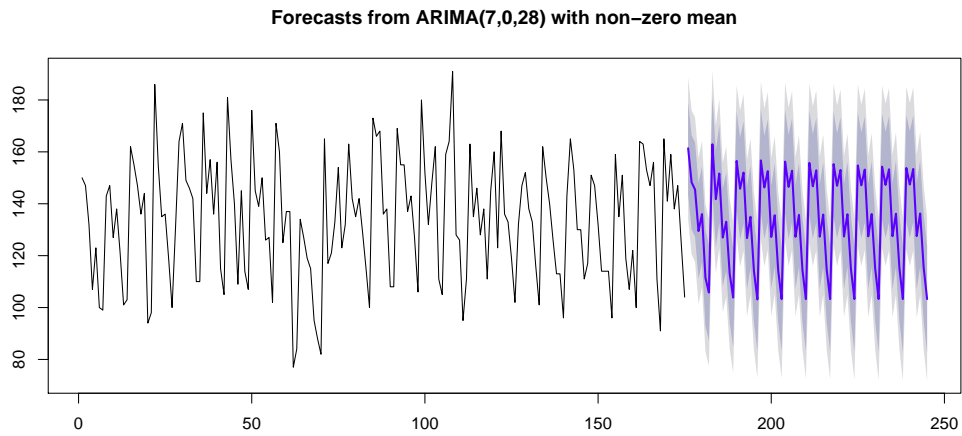


Figure 9: A forecast based on an ARMA(7,28) model fit to the data (Use dataset 3.)

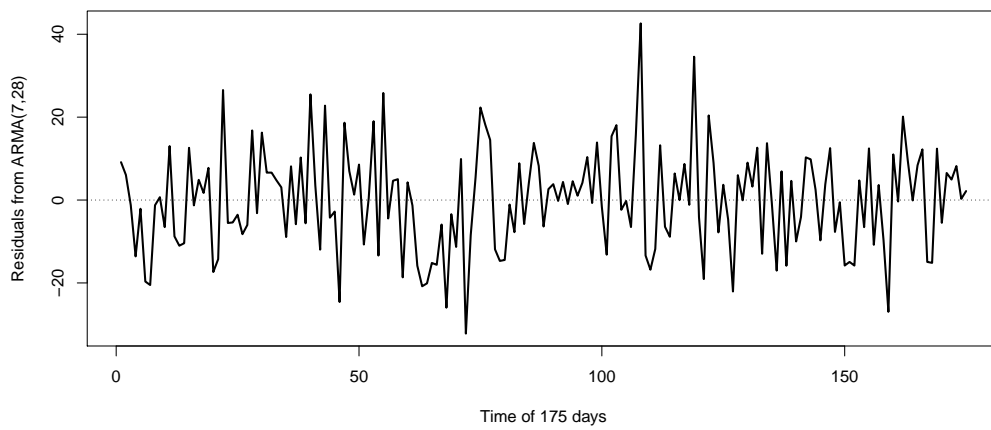


Figure 10: The difference (errors) between the daily totals from the data and the Gaussian model (Use dataset 3.)

3.3. Arrival Pattern Within Days

3.4. Stochastic Variability in the Time-Varying Arrival Process

As we wrote before, it is commonly accepted that the arrival process to an ED can be modeled by a nonhomogeneous Poisson process (NHPP), because the arrivals typically come from the independent medical incidents of many different people, each of whom uses the ED infrequently. Mathematical support is provided by the Poisson superposition theorem; e.g., §11.2 of [13], but that should be verified, as in [9, 10]. Indeed, a moderate level of overdispersion was found before by [14, 15].

Indeed, we have already seen strong stochastic variation in the daily totals that suggests overdispersion relative to a Poisson process. To illustrate unsuspected bunching of arrival that can occur, anecdotally from New York, ED employees report surges of arrivals at public transportation arrival times at the hospital.

Accordingly, we investigated the stochastic variability in the arrival process by (i) estimating the index of dispersion for counts, as in [16, 17], and by performing statistical tests of the NHPP property as in [9, 10]. We briefly summarize the results of our investigations.

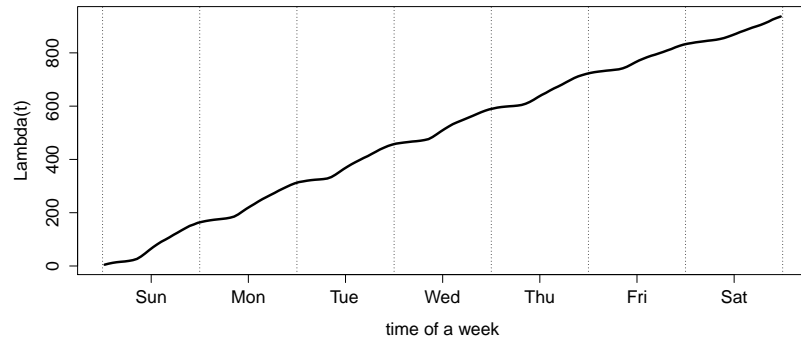
3.4.1. The Index of Dispersion for Counts

The index of dispersion for counts (IDC) is the ratio of the variance to the mean of the arrival counting process, as a function of time. Let $A(t)$ be the number of arrivals in interval $[0, t]$, so that $\{A(t), : t \geq 0\}$ is the arrival counting process. Let $\Lambda(t) \equiv \mathbb{E}[A(t)]$ and $V(t) \equiv \text{Var}(A(t))$ be the mean and variance functions. Then the IDC is $I(t) \equiv V(t)/\Lambda(t)$, $t \geq 0$.

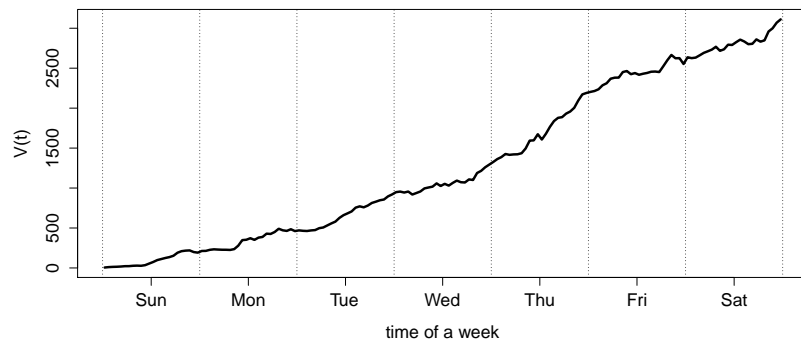
Here we have both week view and day view. In Week view we take $T = 7 * 24 = 168$ hours, and estimate $\Lambda(t)$ and $V(t)$ hourly by taking the 25 weeks as samples, then compute the ratio to estimate $I(t)$. In day view we take $T = 24$ hours, and take the $25 * 7 = 175$ days as samples. In day of week view we take $T = 24$ hours, and take each specific day of week in the 25 weeks (i.e. the sample size is 25 for each day of week).

The week view is in Figure 11. we see that the IDC in Figure 11(c) is increasing. This means that the arrival counting processes in successive days are correlated, thus the variance of the counting process of a week long is larger than the sum of variances of the counting processes of each days. Similarly, if we combine all the days, as shown in Figure 12, the IDC is still increasing significantly.

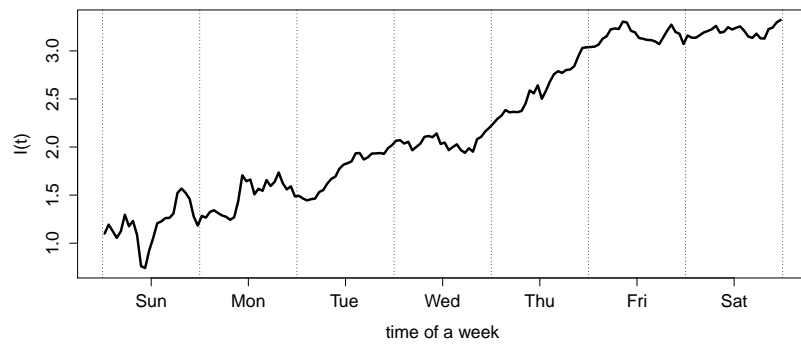
But if we look at the IDC for each day of week separately, as shown in Figure 13, we see that the IDC is much more flat. Figure 13(c) shows that the average of the seven DoW IDC's is about 1.5, which coincide with the regression result for the daily total arrivals with the single-factor model in §3.1 of the main paper.



(a) $\Lambda(t)$

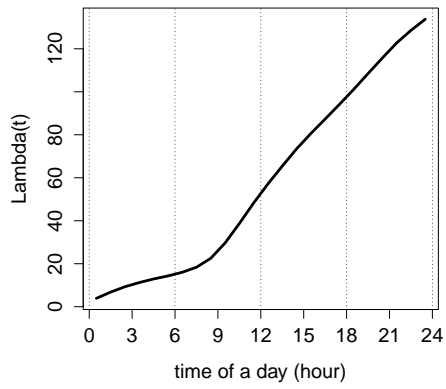


(b) $V(t)$

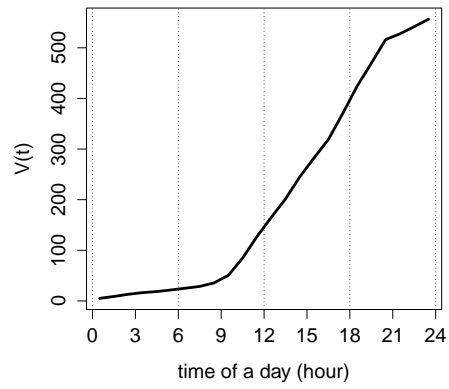


(c) $I(t) = \frac{V(t)}{\Lambda(t)}$

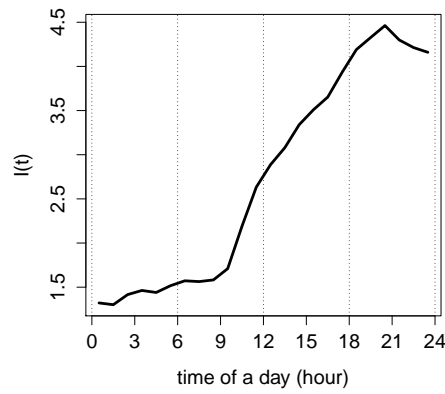
Figure 11: Index of dispersion in week view. (Use data set 3.)



(a) $\Lambda(t)$

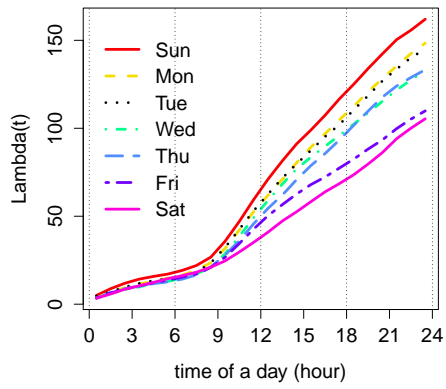


(b) $V(t)$

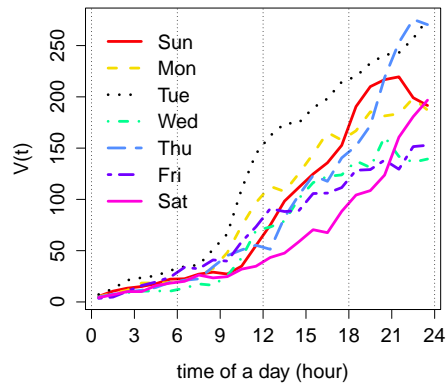


(c) $I(t) = \frac{V(t)}{\Lambda(t)}$

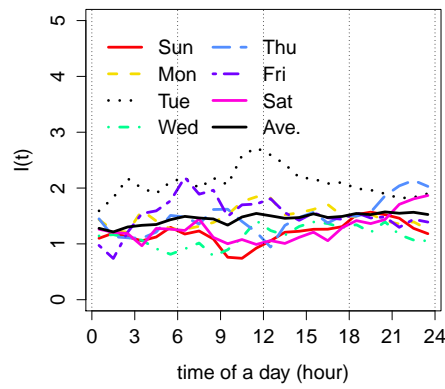
Figure 12: Index of dispersion in day view. (Use data set 3.)



(a) $\Lambda(t)$



(b) $V(t)$



(c) $I(t) = \frac{V(t)}{\Lambda(t)}$

Figure 13: Index of dispersion in day of week view. (Use data set 3.)

3.4.2. Statistical Tests of the NHPP Property

The analysis above indicates that the arrival process is not an NHPP directly, but within a given day, the IDC is like constant about 1.5, which is a little larger than a Poisson Process.

To precisely test the departures from the NHPP assumption, we need a statistical test. Kim and Whitt [10] suggested the conditional uniform KolmogorovSmirnov test (CU KS test) and the Lewis KS test for this purpose. The test results are shown in Table 2. In the test, we divide a day into several time intervals and consider each day of week separately. We regard subintervals of length L as intervals over which the arrival rate might be regarded as constant; i.e., L is the time unit (in hours) over which we might regard the arrival process as a homogeneous Poisson process. Since the data is rounded to the nearest second, we also apply the unrounding by adding iid uniform random variables on $[0, 1]$ second; see [10].

The results in Table 2 indicate that most intervals passed the test. However, in some time periods, like 11 a.m. to 13 p.m., the hypothesis is rejected more frequently. We notice that the unrounding pretreatment does not change much. This presumably is because a second is relatively small in this context.

Int start	Int end	Day of week	N	$L = 1$, raw		$L = 1$, unrounded		$L = 0.5$, raw		$L = 0.5$, unrounded	
				CU	Lewis	CU	Lewis	CU	Lewis	CU	Lewis
0	7	Sun	480	0.67	0.56	0.67	0.54	0.61	0.26	0.63	0.24
0	7	Mon	413	0.51	0.48	0.51	0.49	0.71	0.23	0.72	0.22
0	7	Tues	395	0.11	0.40	0.11	0.43	0.80	0.97	0.79	0.96
0	7	Wed	369	0.59	0.73	0.59	0.73	0.87	0.98	0.87	0.98
0	7	Thurs	356	0.06	0.17	0.06	0.17	0.62	0.54	0.62	0.51
0	7	Fri	384	0.98	0.24	0.98	0.24	0.57	0.60	0.58	0.63
0	7	Sat	405	0.87	0.14	0.87	0.14	0.56	0.07	0.56	0.07
7	9	Sun	188	0.81	0.69	0.81	0.69	0.78	0.65	0.78	0.63
7	9	Mon	176	0.03	0.26	0.03	0.27	0.11	0.78	0.10	0.78
7	9	Tues	192	0.00	0.49	0.00	0.49	0.68	0.25	0.70	0.22
7	9	Wed	150	0.00	0.24	0.00	0.24	0.03	0.69	0.03	0.68
7	9	Thurs	174	0.07	0.52	0.07	0.52	0.11	0.31	0.11	0.29
7	9	Fri	138	0.19	0.84	0.18	0.82	0.30	0.17	0.29	0.17
7	9	Sat	121	0.16	0.13	0.16	0.14	0.85	0.28	0.85	0.28
9	11	Sun	509	0.20	0.03	0.20	0.03	0.30	0.04	0.30	0.03
9	11	Mon	466	0.26	0.03	0.26	0.03	0.40	0.05	0.39	0.04
9	11	Tues	478	0.70	0.05	0.69	0.05	0.05	0.03	0.05	0.04
9	11	Wed	447	0.49	0.15	0.49	0.16	0.39	0.06	0.38	0.06
9	11	Thurs	375	0.31	0.73	0.31	0.74	0.86	0.93	0.85	0.93
9	11	Fri	341	0.70	0.03	0.69	0.03	0.06	0.02	0.06	0.01
9	11	Sat	216	0.09	0.20	0.08	0.20	0.44	0.18	0.44	0.19
11	13	Sun	598	0.10	0.00	0.10	0.00	0.06	0.01	0.06	0.01
11	13	Mon	493	0.24	0.16	0.24	0.14	0.69	0.11	0.71	0.09
11	13	Tues	498	0.13	0.06	0.13	0.06	0.34	0.01	0.33	0.00
11	13	Wed	508	0.57	0.01	0.58	0.01	0.38	0.01	0.37	0.01
11	13	Thurs	456	0.13	0.19	0.13	0.18	0.05	0.10	0.06	0.10
11	13	Fri	394	0.46	0.10	0.45	0.10	0.87	0.03	0.88	0.03
11	13	Sat	281	0.88	0.23	0.88	0.24	0.93	0.12	0.93	0.13
13	15	Sun	502	0.25	0.00	0.25	0.00	0.81	0.00	0.80	0.00
13	15	Mon	462	0.87	0.01	0.87	0.01	0.12	0.01	0.12	0.00
13	15	Tues	430	0.62	0.06	0.63	0.05	0.27	0.16	0.27	0.17
13	15	Wed	448	0.03	0.31	0.03	0.32	0.20	0.43	0.21	0.43
13	15	Thurs	408	0.88	0.13	0.88	0.13	0.80	0.04	0.80	0.05
13	15	Fri	308	0.17	0.75	0.17	0.74	0.07	0.31	0.08	0.32
13	15	Sat	290	0.84	0.26	0.84	0.26	0.70	0.54	0.70	0.53
15	17	Sun	409	0.89	0.04	0.89	0.03	0.74	0.00	0.75	0.00
15	17	Mon	414	0.13	0.89	0.13	0.89	0.04	0.53	0.04	0.50
15	17	Tues	389	0.31	0.73	0.32	0.75	0.90	0.75	0.90	0.74
15	17	Wed	322	0.06	0.56	0.06	0.53	0.17	0.67	0.17	0.68
15	17	Thurs	373	0.20	0.08	0.21	0.08	0.39	0.08	0.4	0.07
15	17	Fri	243	0.31	0.91	0.31	0.92	0.59	0.97	0.58	0.98
15	17	Sat	284	0.57	0.01	0.56	0.01	0.48	0.01	0.49	0.01
17	19	Sun	440	0.27	0.19	0.27	0.18	0.50	0.07	0.48	0.07
17	19	Mon	387	0.95	0.65	0.95	0.65	0.89	0.73	0.88	0.72
17	19	Tues	380	0.55	0.44	0.55	0.44	0.92	0.07	0.91	0.08
17	19	Wed	314	0.54	0.16	0.53	0.17	0.55	0.36	0.56	0.33
17	19	Thurs	401	0.71	0.10	0.72	0.10	0.74	0.05	0.73	0.05
17	19	Fri	254	0.23	0.83	0.23	0.86	0.61	0.12	0.61	0.12
17	19	Sat	243	0.46	0.49	0.45	0.47	0.69	0.01	0.68	0.01
19	21	Sun	431	0.05	0.20	0.05	0.22	0.57	0.10	0.57	0.10
19	21	Mon	394	0.64	0.72	0.63	0.70	0.99	0.64	0.99	0.62
19	21	Tues	410	0.49	0.10	0.48	0.11	0.33	0.42	0.32	0.41
19	21	Wed	324	0.36	0.12	0.36	0.11	0.74	0.19	0.76	0.17
19	21	Thurs	399	0.83	0.00	0.84	0.00	0.68	0.00	0.69	0.00
19	21	Fri	272	0.41	0.69	0.41	0.67	0.67	0.42	0.68	0.41
19	21	Sat	314	0.69	0.77	0.70	0.80	0.58	0.55	0.59	0.53
21	24	Sun	493	0.59	0.03	0.60	0.02	0.82	0.04	0.83	0.04
21	24	Mon	505	0.19	0.01	0.20	0.01	0.96	0.07	0.97	0.08
21	24	Tues	454	0.13	0.21	0.13	0.21	0.47	0.24	0.48	0.24
21	24	Wed	428	0.11	0.98	0.11	0.97	0.93	0.88	0.93	0.9
21	24	Thurs	389	0.13	0.86	0.13	0.80	0.03	0.42	0.04	0.44
21	24	Fri	413	0.33	0.30	0.33	0.30	0.55	0.83	0.54	0.86
21	24	Sat	481	0.22	0.47	0.22	0.45	0.31	0.48	0.3	0.54
Average			371.6	0.40	0.33	0.40	0.33	0.53	0.31	0.53	0.31
# Pass				58	50	58	50	60	46	59	47

Table 2: NHPP test results

3.5. Arrival Processes of the Two Groups: Admitted and Non-Admitted

In Section 2 of the main paper we mentioned that the patients in ED can be divided into two groups according to the admission decision. The non-admitted patients were released after being treated in the ED, while the admitted ones were transferred to one of the internal wards (IW's) of the main hospital. A priori, the two processes are not affected by each other. In other word, we presume that the two separate arrival processes can be regarded as an independent thinning from the whole arrival process.

In Figure 14 we show the arrival rates of the admitted and non-admitted patients for a week. Generally, the shape of the curves are quite similar. The arrival rate of non-admitted patients are almost always higher than the one of admitted patients. Overall, 40% of the arriving patients are admitted.

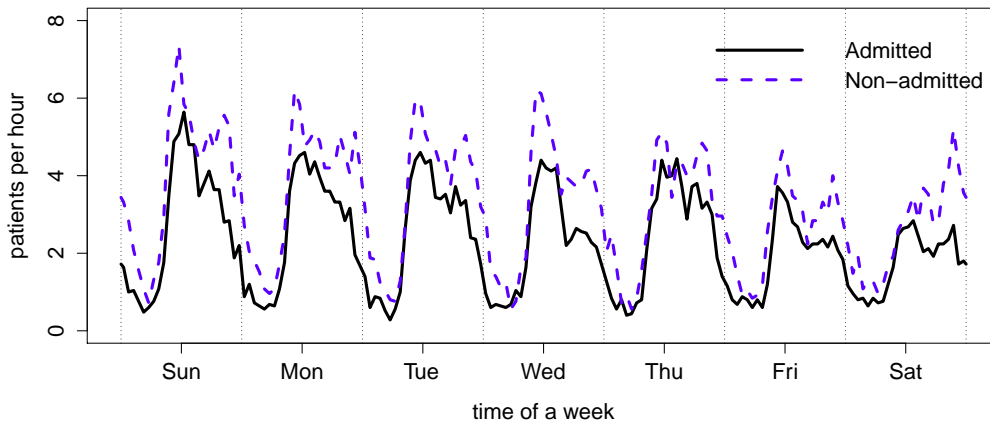


Figure 14: Arrival rates for the admitted and non-admitted patients. (Use data set 5 and 6.)

Further, we look at the proportion of admitted patients in total arrivals for a week in Figure 15. It coincides with Figure 14, but more clearly shows that the proportion of admitted patients is a function of time. Then we want to see if we can combine all the days. In Figure 16(a) we show the estimated proportion of admitted patients by combining all the 175 days. We see that after combining, the line still represents the proportion of admitted patients well for each day of week, thus we think when a patient comes to the ED, with

probability $p(t)$ the patient will be admitted (and with probability $1 - p(t)$ be released), where $p(t)$ is a function of time with period 1 day.

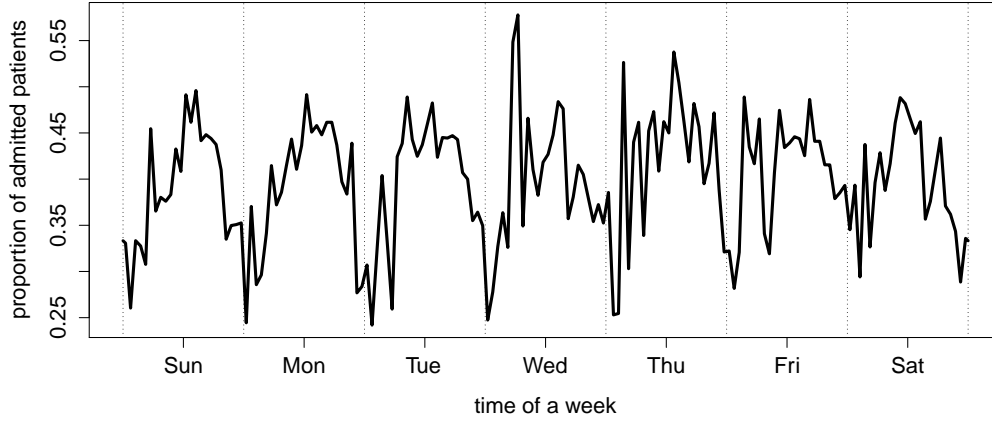


Figure 15: Estimated proportion of admitted patients in arrival process of EIMU for a week. (Use data set 5 and 6.)

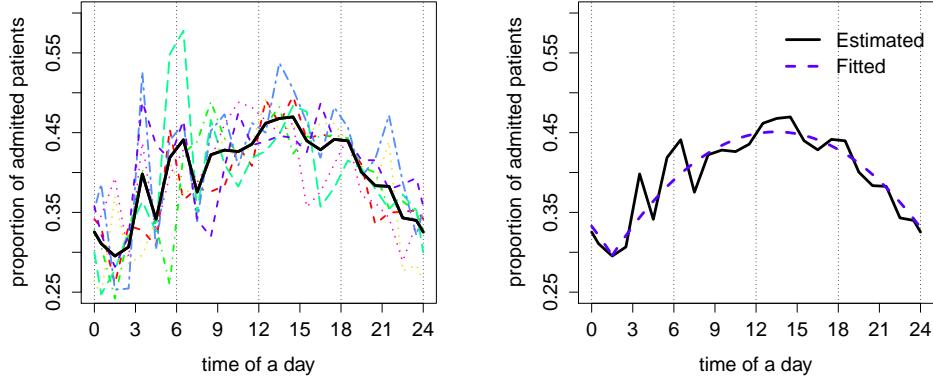
According to Figure 16(a), we fit a quadratic function for $p(t)$ using the method of least squares with a fixed vertex at 2:30 p.m.. The result is shown in Figure 16(b). The expression of the fitted function $\hat{p}(t)$ is

$$\begin{aligned}
 \hat{p}(t) &= f(x) \\
 &= -0.001082x^2 + 0.02914x + 0.2548015 \\
 &= -0.001082(x - 13.5)^2 + 0.451996,
 \end{aligned} \tag{2}$$

where $x = ((t - 1.5) \bmod 24) + 1.5$ and $t \in [0, 24]$.

3.6. Summary: Full Model of the ED Arrival Process

Repeating the main paper, we combine the analysis in the previous subsections to develop a full arrival process model that can be used in simulation studies. First, the daily totals for the number of arrivals are modeled as independent random variables with a Gaussian distribution, as determined by the single-factor Gaussian model in §3.1 if the main paper. Then, given the daily totals, the arrival process is modelled as an NHPP, which means that



(a) Estimated proportion of admitted patients in arrival process of EIMU for a day combining all days together (black solid line) and the proportions of admitted patients for each day of week. (b) Fitting the Estimated proportion of admitted patients in arrival process of EIMU for a day with a quadratic function.

Figure 16: Proportion of admitted patients in the arrival process of EIMU for a day. (Use data set 5 and 6.)

the given random daily number of arrivals are treated as i.i.d. random variables over the entire day with a pdf proportional to the estimated arrival rate function for that day. We refer to that arrival process model as M_t^T . Finally, a patient that arrives at time t is admitted with probability $p(t)$, estimated by the quadratic function above. We conduct simulation experiments using the model in §6.

4. Length of Stay

In this section, we investigate the LoS distribution for the ED. We find the LoS is time-varying. Particularly, there is a midnight surge in the departure process. It tends to clear all the patients that arrived early in the day. Even for patients who arrived in the afternoon or evening, there exist a slight departure surge before midnight. We will show this time view in §5. In this data, two key effects are confounded: (i) service time (i.e., service requirement) and (ii) extra congestion (i.e., waiting, because of congestion). We do not see these as separate directly from the data, but we try to recognize them in §9.

4.1. General LoS Distribution

In general, we know that the mean LoS for patients in ED (EIMU) is 4.10 hour, which is relatively short compared to a day. But if we look at the histogram and ECDF of LoS in Figure 17 and 18, we see that there are also patients, though not many, who have relatively long LoS.

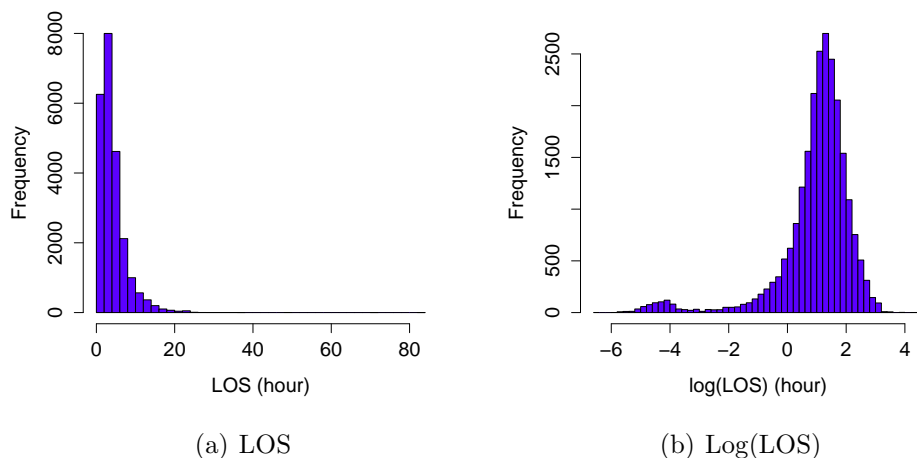


Figure 17: Histogram of LOS for EIMU. (Use data set 3.)

4.2. Failure of the $G_t/GI/\infty$ Aggregate Model

4.3. The Time-Varying LoS Distribution

At first we were not aware of the time-varying structure of LoS. In our study the patient LoS is given by the difference of the exit time and the enter time of the patient (See Section 2 in the main paper). We only know when did the patients come and when the patients were released, but we know nothing about what happened between. In other word, we do not know what proportion of the LoS is the waiting time and how long is the service time.

We tried an $M_t/GI/\infty$ model but the predicted number of patients in the system is not close to the reality. This made us to question the assumptions of the model, in particular, the assumption that the service times are iid.

To see this in a simple way, we plot the box-plot of LoS of for each hour. First we look at it in week view in Figure 19. Though not obvious in week

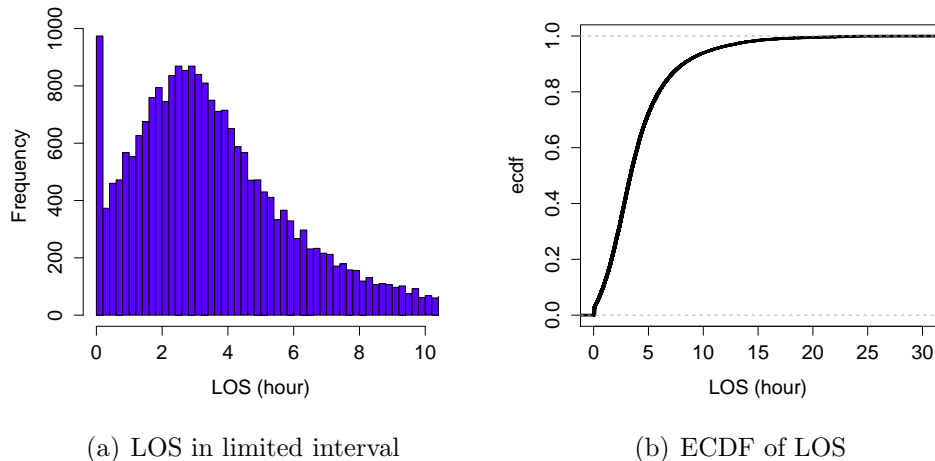


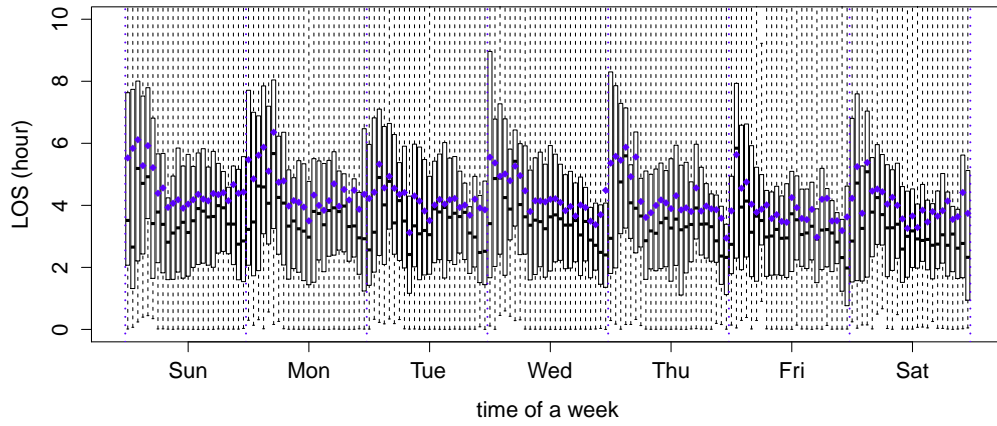
Figure 18: Histogram of LOS limited to interval $[0, 10]$ and the empirical cdf for EIMU. (Use data set 3.)

view, we see a time-varying structure within a day. We see more clearly from the same plot for a day in Figure 20(a). In Figure 20(a) we see that the mean LoS is large in the early morning and is decreasing until 9 a.m., then it keeps like constant though the day time. The median of LoS is more interesting. It is also large in the early morning and decreasing until 9 a.m., then it keeps like constant until 7 p.m.. From 7 p.m. to midnight, it decreases, and at midnight it reaches the bottom. After midnight, it rapidly increases to high level.

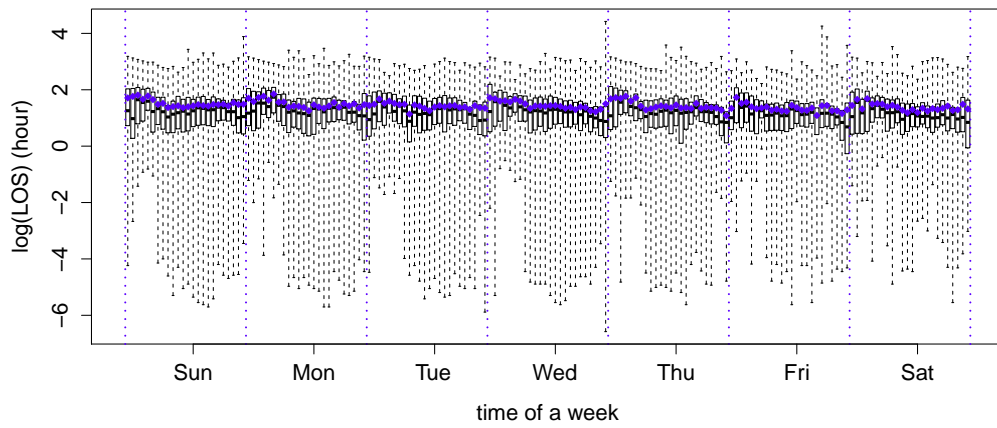
We make several tables to see the time-varying length of stay more clearly. Table 3, 4 and 5 show the entire \bar{X} matrix as defined in the main paper. We use different fonts and grey backgrounds to emphasize the midnight push-out. Table 6, 7 and 8 show the normalized \bar{X} matrix where we normalized each row of \bar{X} into a probability distribution. We can see the significant difference among the 24 distributions. Finally Table 9, 10 and 11 show the complementary cumulative distribution functions, which is just 1 subtracts the cumulative summation of the normalized \bar{X} matrix. It gives us another view of the time-varying distributions of length of stay.

4.4. The LoS of the Two Groups

4.5. The LoS Model and Occupancy

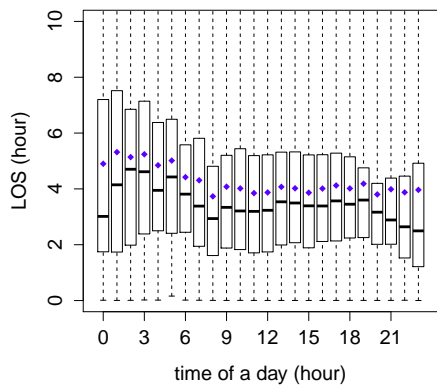


(a) LoS by time.

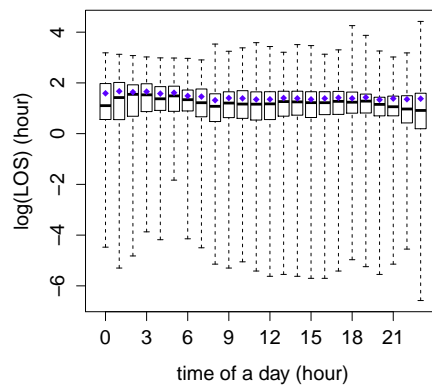


(b) $\log(\text{LoS})$ by time.

Figure 19: Time view of LoS. The blue dots are means and the black bars are medians. (Use data set 3.)



(a) LoS by time.



(b) $\log(\text{LoS})$ by time.

Figure 20: Time view of LoS. (Use data set 3.)

	1	2	3	4	5	6	7	8
0	0.194	0.160	0.120	0.063	0.086	0.051	0.057	0.149
1	0.531	0.451	0.297	0.234	0.143	0.171	0.131	0.246
2	0.891	0.486	0.314	0.189	0.194	0.154	0.234	0.366
3	0.554	0.274	0.211	0.171	0.286	0.160	0.314	0.417
4	0.280	0.131	0.280	0.274	0.217	0.183	0.263	0.337
5	0.154	0.131	0.297	0.223	0.200	0.183	0.263	0.171
6	0.137	0.337	0.280	0.177	0.143	0.171	0.189	0.194
7	0.246	0.206	0.160	0.149	0.160	0.091	0.091	0.120
8	0.171	0.217	0.177	0.171	0.063	0.057	0.023	0.051
9	0.166	0.160	0.091	0.120	0.040	0.029	0.029	0.103
10	0.189	0.086	0.057	0.034	0.040	0.034	0.006	0.051
11	0.103	0.074	0.086	0.040	0.029	0.051	0.023	0.017
12	0.063	0.017	0.029	0.011	0.006	0.011	0.017	0.034
13	0.074	0.017	0.006	0.023	0.011	0.000	0.011	0.017
14	0.006	0.017	0.017	0.006	0.000	0.000	0.000	0.006
15	0.006	0.017	0.011	0.006	0.006	0.011	0.006	0.006
16	0.006	0.006	0.000	0.000	0.000	0.000	0.000	0.057
17	0.000	0.000	0.000	0.006	0.000	0.000	0.034	0.000
18	0.000	0.000	0.006	0.000	0.006	0.040	0.000	0.006
19	0.000	0.000	0.000	0.000	0.046	0.000	0.006	0.000
20	0.000	0.000	0.000	0.040	0.000	0.006	0.000	0.000
21	0.000	0.000	0.057	0.000	0.000	0.000	0.000	0.000
22	0.000	0.120	0.000	0.000	0.000	0.000	0.000	0.000
23	0.114	0.000	0.000	0.000	0.000	0.000	0.000	0.000
24	0.000	0.000	0.000	0.000	0.000	0.000	0.000	0.000
25	0.006	0.000	0.000	0.000	0.000	0.000	0.000	0.000
26	0.000	0.000	0.000	0.000	0.000	0.000	0.000	0.000
27	0.000	0.000	0.000	0.000	0.000	0.000	0.000	0.000
28	0.000	0.000	0.000	0.000	0.000	0.000	0.000	0.000
29	0.000	0.000	0.000	0.000	0.000	0.000	0.000	0.000
30	0.000	0.000	0.000	0.000	0.000	0.000	0.000	0.000
31	0.000	0.000	0.000	0.000	0.000	0.000	0.000	0.000
32	0.000	0.000	0.000	0.000	0.000	0.000	0.000	0.000
33	0.000	0.000	0.000	0.000	0.000	0.000	0.000	0.000
34	0.000	0.000	0.000	0.000	0.000	0.000	0.000	0.000
35	0.000	0.000	0.000	0.000	0.000	0.000	0.000	0.000
36	0.000	0.000	0.000	0.000	0.000	0.000	0.000	0.000

24
Table 3: \bar{X}^T part 1. (Use data set 4).

	9	10	11	12	13	14	15	16
0	0.434	0.526	0.709	0.789	0.771	0.531	0.743	0.771
1	0.491	0.817	1.069	1.263	1.194	1.006	0.680	0.640
2	0.709	1.194	1.560	1.543	1.446	1.211	1.114	1.017
3	0.754	1.177	1.691	1.554	1.286	1.343	1.549	1.314
4	0.623	1.040	1.114	1.154	1.331	1.257	1.171	1.080
5	0.320	0.669	0.703	1.257	0.840	1.011	0.874	0.709
6	0.217	0.411	0.697	0.657	0.583	0.594	0.651	0.549
7	0.154	0.400	0.394	0.366	0.474	0.423	0.343	0.314
8	0.171	0.246	0.274	0.257	0.263	0.211	0.211	0.497
9	0.074	0.131	0.211	0.206	0.211	0.137	0.446	0.097
10	0.017	0.109	0.149	0.097	0.069	0.383	0.051	0.029
11	0.023	0.080	0.051	0.086	0.269	0.034	0.051	0.023
12	0.029	0.029	0.046	0.246	0.051	0.011	0.011	0.023
13	0.006	0.023	0.366	0.006	0.029	0.011	0.006	0.006
14	0.000	0.234	0.011	0.023	0.011	0.000	0.000	0.006
15	0.126	0.006	0.000	0.017	0.000	0.000	0.011	0.006
16	0.000	0.006	0.006	0.006	0.011	0.017	0.011	0.000
17	0.000	0.006	0.000	0.006	0.006	0.017	0.011	0.017
18	0.000	0.000	0.000	0.000	0.000	0.017	0.011	0.011
19	0.000	0.000	0.000	0.000	0.006	0.011	0.017	0.011
20	0.000	0.000	0.006	0.000	0.000	0.011	0.029	0.000
21	0.000	0.000	0.000	0.006	0.011	0.006	0.000	0.017
22	0.000	0.000	0.000	0.006	0.000	0.000	0.011	0.000
23	0.000	0.000	0.006	0.011	0.006	0.006	0.000	0.006
24	0.000	0.006	0.000	0.000	0.000	0.011	0.000	0.000
25	0.000	0.000	0.000	0.000	0.000	0.000	0.000	0.006
26	0.000	0.006	0.000	0.000	0.000	0.000	0.000	0.000
27	0.000	0.000	0.000	0.006	0.000	0.000	0.000	0.006
28	0.000	0.000	0.000	0.000	0.000	0.000	0.000	0.000
29	0.000	0.000	0.000	0.000	0.000	0.000	0.000	0.000
30	0.006	0.000	0.006	0.000	0.006	0.000	0.000	0.000
31	0.000	0.000	0.000	0.000	0.006	0.000	0.000	0.000
32	0.000	0.000	0.000	0.000	0.000	0.000	0.000	0.006
33	0.000	0.000	0.000	0.000	0.000	0.000	0.006	0.000
34	0.006	0.000	0.000	0.000	0.000	0.000	0.000	0.000
35	0.000	0.000	0.000	0.000	0.000	0.000	0.000	0.000
36	0.000	0.000	0.000	0.006	0.000	0.000	0.000	0.000

25
Table 4: \bar{X}^T part 2. (Use data set 4).

	17	18	19	20	21	22	23	24
0	0.480	0.337	0.349	0.291	0.326	0.366	0.229	0.989
1	0.640	0.749	0.731	0.680	0.891	0.760	1.549	0.520
2	1.057	0.983	0.971	1.263	1.160	1.903	1.051	1.103
3	1.326	1.206	1.497	1.354	2.309	1.309	0.977	0.817
4	1.029	1.291	1.029	1.829	0.943	1.023	0.617	0.366
5	0.657	0.669	1.331	0.657	0.606	0.440	0.269	0.223
6	0.451	0.851	0.366	0.417	0.246	0.171	0.114	0.131
7	0.617	0.189	0.229	0.177	0.103	0.114	0.166	0.103
8	0.120	0.137	0.171	0.091	0.069	0.131	0.029	0.200
9	0.103	0.080	0.034	0.063	0.040	0.086	0.223	0.171
10	0.063	0.046	0.040	0.029	0.046	0.114	0.120	0.126
11	0.040	0.011	0.023	0.040	0.091	0.143	0.154	0.126
12	0.011	0.011	0.023	0.074	0.080	0.137	0.131	0.097
13	0.023	0.023	0.034	0.114	0.057	0.109	0.069	0.080
14	0.011	0.029	0.063	0.040	0.103	0.091	0.046	0.057
15	0.023	0.040	0.023	0.040	0.034	0.057	0.029	0.017
16	0.011	0.040	0.029	0.063	0.046	0.034	0.029	0.011
17	0.023	0.034	0.023	0.029	0.046	0.029	0.029	0.023
18	0.011	0.006	0.017	0.029	0.006	0.006	0.000	0.000
19	0.017	0.040	0.011	0.017	0.000	0.000	0.006	0.006
20	0.011	0.017	0.006	0.023	0.006	0.000	0.000	0.000
21	0.011	0.000	0.000	0.000	0.000	0.011	0.000	0.000
22	0.006	0.000	0.006	0.000	0.000	0.000	0.000	0.000
23	0.006	0.006	0.006	0.000	0.000	0.000	0.006	0.000
24	0.000	0.000	0.000	0.000	0.000	0.000	0.006	0.011
25	0.000	0.000	0.000	0.000	0.000	0.000	0.000	0.000
26	0.000	0.006	0.000	0.000	0.006	0.000	0.000	0.000
27	0.000	0.006	0.000	0.000	0.000	0.000	0.000	0.000
28	0.000	0.000	0.000	0.000	0.000	0.000	0.000	0.000
29	0.000	0.000	0.000	0.000	0.000	0.000	0.000	0.000
30	0.000	0.000	0.000	0.000	0.000	0.000	0.000	0.000
31	0.000	0.000	0.000	0.000	0.000	0.000	0.000	0.000
32	0.000	0.000	0.000	0.000	0.000	0.000	0.000	0.000
33	0.000	0.000	0.000	0.000	0.000	0.000	0.000	0.000
34	0.000	0.000	0.000	0.000	0.000	0.000	0.000	0.000
35	0.000	0.000	0.000	0.000	0.000	0.000	0.000	0.000
36	0.000	0.000	0.000	0.000	0.000	0.000	0.000	0.006

26
Table 5: \bar{X}^T part 3. (Use data set 4).

	1	2	3	4	5	6	7	8
0	0.0499	0.0550	0.0481	0.0324	0.0512	0.0366	0.0337	0.0633
1	0.1366	0.1552	0.1190	0.1209	0.0853	0.1220	0.0774	0.1046
2	0.2291	0.1670	0.1259	0.0973	0.1160	0.1098	0.1380	0.1557
3	0.1424	0.0943	0.0847	0.0885	0.1706	0.1138	0.1852	0.1776
4	0.0720	0.0452	0.1121	0.1416	0.1297	0.1301	0.1549	0.1436
5	0.0396	0.0452	0.1190	0.1150	0.1195	0.1301	0.1549	0.0730
6	0.0352	0.1159	0.1121	0.0914	0.0853	0.1220	0.1111	0.0827
7	0.0631	0.0707	0.0641	0.0767	0.0956	0.0650	0.0539	0.0511
8	0.0441	0.0747	0.0709	0.0885	0.0375	0.0407	0.0135	0.0219
9	0.0426	0.0550	0.0366	0.0619	0.0239	0.0203	0.0168	0.0438
10	0.0485	0.0295	0.0229	0.0177	0.0239	0.0244	0.0034	0.0219
11	0.0264	0.0255	0.0343	0.0206	0.0171	0.0366	0.0135	0.0073
12	0.0162	0.0059	0.0114	0.0059	0.0034	0.0081	0.0101	0.0146
13	0.0191	0.0059	0.0023	0.0118	0.0068	0.0000	0.0067	0.0073
14	0.0015	0.0059	0.0069	0.0029	0.0000	0.0000	0.0000	0.0024
15	0.0015	0.0059	0.0046	0.0029	0.0034	0.0081	0.0034	0.0024
16	0.0015	0.0020	0.0000	0.0000	0.0000	0.0000	0.0000	0.0243
17	0.0000	0.0000	0.0000	0.0029	0.0000	0.0000	0.0202	0.0000
18	0.0000	0.0000	0.0023	0.0000	0.0034	0.0285	0.0000	0.0024
19	0.0000	0.0000	0.0000	0.0000	0.0273	0.0000	0.0034	0.0000
20	0.0000	0.0000	0.0000	0.0206	0.0000	0.0041	0.0000	0.0000
21	0.0000	0.0000	0.0229	0.0000	0.0000	0.0000	0.0000	0.0000
22	0.0000	0.0413	0.0000	0.0000	0.0000	0.0000	0.0000	0.0000
23	0.0294	0.0000	0.0000	0.0000	0.0000	0.0000	0.0000	0.0000
24	0.0000	0.0000	0.0000	0.0000	0.0000	0.0000	0.0000	0.0000
25	0.0015	0.0000	0.0000	0.0000	0.0000	0.0000	0.0000	0.0000
26	0.0000	0.0000	0.0000	0.0000	0.0000	0.0000	0.0000	0.0000
27	0.0000	0.0000	0.0000	0.0000	0.0000	0.0000	0.0000	0.0000
28	0.0000	0.0000	0.0000	0.0000	0.0000	0.0000	0.0000	0.0000
29	0.0000	0.0000	0.0000	0.0000	0.0000	0.0000	0.0000	0.0000
30	0.0000	0.0000	0.0000	0.0000	0.0000	0.0000	0.0000	0.0000
31	0.0000	0.0000	0.0000	0.0000	0.0000	0.0000	0.0000	0.0000
32	0.0000	0.0000	0.0000	0.0000	0.0000	0.0000	0.0000	0.0000
33	0.0000	0.0000	0.0000	0.0000	0.0000	0.0000	0.0000	0.0000
34	0.0000	0.0000	0.0000	0.0000	0.0000	0.0000	0.0000	0.0000
35	0.0000	0.0000	0.0000	0.0000	0.0000	0.0000	0.0000	0.0000
36	0.0000	0.0000	0.0000	0.0000	0.0000	0.0000	0.0000	0.0000

27

Table 6: Normalized \bar{X}^T matrix part 1. Each column is a probability vector. (Use data set 4.)

	9	10	11	12	13	14	15	16
0	0.1044	0.0739	0.0781	0.0824	0.0869	0.0643	0.0927	0.1077
1	0.1181	0.1149	0.1178	0.1320	0.1345	0.1217	0.0849	0.0894
2	0.1703	0.1679	0.1720	0.1613	0.1628	0.1466	0.1391	0.1421
3	0.1813	0.1655	0.1865	0.1625	0.1448	0.1625	0.1933	0.1836
4	0.1497	0.1462	0.1229	0.1207	0.1499	0.1521	0.1462	0.1508
5	0.0769	0.0940	0.0775	0.1314	0.0946	0.1224	0.1091	0.0990
6	0.0522	0.0578	0.0769	0.0687	0.0656	0.0719	0.0813	0.0766
7	0.0371	0.0562	0.0435	0.0382	0.0534	0.0512	0.0428	0.0439
8	0.0412	0.0345	0.0302	0.0269	0.0296	0.0256	0.0264	0.0694
9	0.0179	0.0185	0.0233	0.0215	0.0238	0.0166	0.0556	0.0136
10	0.0041	0.0153	0.0164	0.0102	0.0077	0.0463	0.0064	0.0040
11	0.0055	0.0112	0.0057	0.0090	0.0302	0.0041	0.0064	0.0032
12	0.0069	0.0040	0.0050	0.0257	0.0058	0.0014	0.0014	0.0032
13	0.0014	0.0032	0.0403	0.0006	0.0032	0.0014	0.0007	0.0008
14	0.0000	0.0329	0.0013	0.0024	0.0013	0.0000	0.0000	0.0008
15	0.0302	0.0008	0.0000	0.0018	0.0000	0.0000	0.0014	0.0008
16	0.0000	0.0008	0.0006	0.0006	0.0013	0.0021	0.0014	0.0000
17	0.0000	0.0008	0.0000	0.0006	0.0006	0.0021	0.0014	0.0024
18	0.0000	0.0000	0.0000	0.0000	0.0000	0.0021	0.0014	0.0016
19	0.0000	0.0000	0.0000	0.0000	0.0006	0.0014	0.0021	0.0016
20	0.0000	0.0000	0.0006	0.0000	0.0000	0.0014	0.0036	0.0000
21	0.0000	0.0000	0.0000	0.0006	0.0013	0.0007	0.0000	0.0024
22	0.0000	0.0000	0.0000	0.0006	0.0000	0.0000	0.0014	0.0000
23	0.0000	0.0000	0.0006	0.0012	0.0006	0.0007	0.0000	0.0008
24	0.0000	0.0008	0.0000	0.0000	0.0000	0.0014	0.0000	0.0000
25	0.0000	0.0000	0.0000	0.0000	0.0000	0.0000	0.0000	0.0008
26	0.0000	0.0008	0.0000	0.0000	0.0000	0.0000	0.0000	0.0000
27	0.0000	0.0000	0.0000	0.0006	0.0000	0.0000	0.0000	0.0008
28	0.0000	0.0000	0.0000	0.0000	0.0000	0.0000	0.0000	0.0000
29	0.0000	0.0000	0.0000	0.0000	0.0000	0.0000	0.0000	0.0000
30	0.0014	0.0000	0.0006	0.0000	0.0006	0.0000	0.0000	0.0000
31	0.0000	0.0000	0.0000	0.0000	0.0006	0.0000	0.0000	0.0000
32	0.0000	0.0000	0.0000	0.0000	0.0000	0.0000	0.0000	0.0008
33	0.0000	0.0000	0.0000	0.0000	0.0000	0.0000	0.0007	0.0000
34	0.0014	0.0000	0.0000	0.0000	0.0000	0.0000	0.0000	0.0000
35	0.0000	0.0000	0.0000	0.0000	0.0000	0.0000	0.0000	0.0000
36	0.0000	0.0000	0.0000	0.0006	0.0000	0.0000	0.0000	0.0000

Table 7: Normalized \bar{X}^T matrix part 2. Each column is a probability vector. (Use data set 4.)

	17	18	19	20	21	22	23	24
0	0.0711	0.0495	0.0497	0.0398	0.0452	0.0520	0.0391	0.1907
1	0.0948	0.1100	0.1043	0.0929	0.1236	0.1080	0.2649	0.1003
2	0.1566	0.1444	0.1385	0.1725	0.1609	0.2705	0.1799	0.2128
3	0.1964	0.1772	0.2135	0.1850	0.3201	0.1860	0.1672	0.1577
4	0.1524	0.1898	0.1467	0.2498	0.1307	0.1454	0.1056	0.0706
5	0.0974	0.0982	0.1899	0.0898	0.0840	0.0626	0.0459	0.0430
6	0.0669	0.1251	0.0522	0.0570	0.0341	0.0244	0.0196	0.0254
7	0.0914	0.0277	0.0326	0.0242	0.0143	0.0162	0.0283	0.0198
8	0.0178	0.0202	0.0244	0.0125	0.0095	0.0187	0.0049	0.0386
9	0.0152	0.0118	0.0049	0.0086	0.0055	0.0122	0.0381	0.0331
10	0.0093	0.0067	0.0057	0.0039	0.0063	0.0162	0.0205	0.0243
11	0.0059	0.0017	0.0033	0.0055	0.0127	0.0203	0.0264	0.0243
12	0.0017	0.0017	0.0033	0.0101	0.0111	0.0195	0.0225	0.0187
13	0.0034	0.0034	0.0049	0.0156	0.0079	0.0154	0.0117	0.0154
14	0.0017	0.0042	0.0090	0.0055	0.0143	0.0130	0.0078	0.0110
15	0.0034	0.0059	0.0033	0.0055	0.0048	0.0081	0.0049	0.0033
16	0.0017	0.0059	0.0041	0.0086	0.0063	0.0049	0.0049	0.0022
17	0.0034	0.0050	0.0033	0.0039	0.0063	0.0041	0.0049	0.0044
18	0.0017	0.0008	0.0024	0.0039	0.0008	0.0008	0.0000	0.0000
19	0.0025	0.0059	0.0016	0.0023	0.0000	0.0000	0.0010	0.0011
20	0.0017	0.0025	0.0008	0.0031	0.0008	0.0000	0.0000	0.0000
21	0.0017	0.0000	0.0000	0.0000	0.0000	0.0016	0.0000	0.0000
22	0.0008	0.0000	0.0008	0.0000	0.0000	0.0000	0.0000	0.0000
23	0.0008	0.0008	0.0008	0.0000	0.0000	0.0000	0.0010	0.0000
24	0.0000	0.0000	0.0000	0.0000	0.0000	0.0000	0.0010	0.0022
25	0.0000	0.0000	0.0000	0.0000	0.0000	0.0000	0.0000	0.0000
26	0.0000	0.0008	0.0000	0.0000	0.0008	0.0000	0.0000	0.0000
27	0.0000	0.0008	0.0000	0.0000	0.0000	0.0000	0.0000	0.0000
28	0.0000	0.0000	0.0000	0.0000	0.0000	0.0000	0.0000	0.0000
29	0.0000	0.0000	0.0000	0.0000	0.0000	0.0000	0.0000	0.0000
30	0.0000	0.0000	0.0000	0.0000	0.0000	0.0000	0.0000	0.0000
31	0.0000	0.0000	0.0000	0.0000	0.0000	0.0000	0.0000	0.0000
32	0.0000	0.0000	0.0000	0.0000	0.0000	0.0000	0.0000	0.0000
33	0.0000	0.0000	0.0000	0.0000	0.0000	0.0000	0.0000	0.0000
34	0.0000	0.0000	0.0000	0.0000	0.0000	0.0000	0.0000	0.0000
35	0.0000	0.0000	0.0000	0.0000	0.0000	0.0000	0.0000	0.0000
36	0.0000	0.0000	0.0000	0.0000	0.0000	0.0000	0.0000	0.0011

Table 8: Normalized \bar{X}^T matrix part 3. Each column is a probability vector. (Use data set 4.)

	1	2	3	4	5	6	7	8
0	0.9501	0.9450	0.9519	0.9676	0.9488	0.9634	0.9663	0.9367
1	0.8135	0.7898	0.8330	0.8466	0.8635	0.8415	0.8889	0.8321
2	0.5844	0.6228	0.7071	0.7493	0.7474	0.7317	0.7508	0.6764
3	0.4420	0.5285	0.6224	0.6608	0.5768	0.6179	0.5657	0.4988
4	0.3700	0.4833	0.5103	0.5192	0.4471	0.4878	0.4108	0.3552
5	0.3304	0.4381	0.3913	0.4041	0.3276	0.3577	0.2559	0.2822
6	0.2952	0.3222	0.2792	0.3127	0.2423	0.2358	0.1448	0.1995
7	0.2320	0.2515	0.2151	0.2360	0.1468	0.1707	0.0909	0.1484
8	0.1880	0.1768	0.1442	0.1475	0.1092	0.1301	0.0774	0.1265
9	0.1454	0.1218	0.1076	0.0855	0.0853	0.1098	0.0606	0.0827
10	0.0969	0.0923	0.0847	0.0678	0.0614	0.0854	0.0572	0.0608
11	0.0705	0.0668	0.0503	0.0472	0.0444	0.0488	0.0438	0.0535
12	0.0543	0.0609	0.0389	0.0413	0.0410	0.0407	0.0337	0.0389
13	0.0352	0.0550	0.0366	0.0295	0.0341	0.0407	0.0269	0.0316
14	0.0338	0.0491	0.0297	0.0265	0.0341	0.0407	0.0269	0.0292
15	0.0323	0.0432	0.0252	0.0236	0.0307	0.0325	0.0236	0.0268
16	0.0308	0.0413	0.0252	0.0236	0.0307	0.0325	0.0236	0.0024
17	0.0308	0.0413	0.0252	0.0206	0.0307	0.0325	0.0034	0.0024
18	0.0308	0.0413	0.0229	0.0206	0.0273	0.0041	0.0034	0.0000
19	0.0308	0.0413	0.0229	0.0206	0.0000	0.0041	0.0000	0.0000
20	0.0308	0.0413	0.0229	0.0000	0.0000	0.0000	0.0000	0.0000
21	0.0308	0.0413	0.0000	0.0000	0.0000	0.0000	0.0000	0.0000
22	0.0308	0.0000	0.0000	0.0000	0.0000	0.0000	0.0000	0.0000
23	0.0015	0.0000	0.0000	0.0000	0.0000	0.0000	0.0000	0.0000
24	0.0015	0.0000	0.0000	0.0000	0.0000	0.0000	0.0000	0.0000
25	0.0000	0.0000	0.0000	0.0000	0.0000	0.0000	0.0000	0.0000
26	0.0000	0.0000	0.0000	0.0000	0.0000	0.0000	0.0000	0.0000
27	0.0000	0.0000	0.0000	0.0000	0.0000	0.0000	0.0000	0.0000
28	0.0000	0.0000	0.0000	0.0000	0.0000	0.0000	0.0000	0.0000
29	0.0000	0.0000	0.0000	0.0000	0.0000	0.0000	0.0000	0.0000
30	0.0000	0.0000	0.0000	0.0000	0.0000	0.0000	0.0000	0.0000
31	0.0000	0.0000	0.0000	0.0000	0.0000	0.0000	0.0000	0.0000
32	0.0000	0.0000	0.0000	0.0000	0.0000	0.0000	0.0000	0.0000
33	0.0000	0.0000	0.0000	0.0000	0.0000	0.0000	0.0000	0.0000
34	0.0000	0.0000	0.0000	0.0000	0.0000	0.0000	0.0000	0.0000
35	0.0000	0.0000	0.0000	0.0000	0.0000	0.0000	0.0000	0.0000
36	0.0000	0.0000	0.0000	0.0000	0.0000	0.0000	0.0000	0.0000

30
Table 9: CCDF of TV LOS part 1. Each column is the CCDF of LOS for patients entered in time period of column index, e.g. column 1 is the CCDF of LOS for patients entered in 00:00-01:00 (Use data set 4.)

	9	10	11	12	13	14	15	16
0	0.8956	0.9261	0.9219	0.9176	0.9131	0.9357	0.9073	0.8923
1	0.7775	0.8112	0.8040	0.7855	0.7786	0.8140	0.8224	0.8029
2	0.6071	0.6434	0.6320	0.6243	0.6158	0.6674	0.6833	0.6608
3	0.4258	0.4779	0.4455	0.4618	0.4710	0.5048	0.4900	0.4773
4	0.2761	0.3317	0.3226	0.3411	0.3211	0.3527	0.3438	0.3264
5	0.1992	0.2378	0.2451	0.2097	0.2265	0.2303	0.2347	0.2275
6	0.1470	0.1799	0.1682	0.1410	0.1609	0.1584	0.1534	0.1508
7	0.1099	0.1237	0.1248	0.1027	0.1075	0.1072	0.1106	0.1069
8	0.0687	0.0892	0.0945	0.0759	0.0779	0.0816	0.0842	0.0375
9	0.0508	0.0707	0.0712	0.0544	0.0541	0.0650	0.0285	0.0239
10	0.0467	0.0554	0.0548	0.0442	0.0463	0.0187	0.0221	0.0200
11	0.0412	0.0442	0.0491	0.0352	0.0161	0.0145	0.0157	0.0168
12	0.0343	0.0402	0.0441	0.0096	0.0103	0.0131	0.0143	0.0136
13	0.0330	0.0369	0.0038	0.0090	0.0071	0.0118	0.0136	0.0128
14	0.0330	0.0040	0.0025	0.0066	0.0058	0.0118	0.0136	0.0120
15	0.0027	0.0032	0.0025	0.0048	0.0058	0.0118	0.0121	0.0112
16	0.0027	0.0024	0.0019	0.0042	0.0045	0.0097	0.0107	0.0112
17	0.0027	0.0016	0.0019	0.0036	0.0039	0.0076	0.0093	0.0088
18	0.0027	0.0016	0.0019	0.0036	0.0039	0.0055	0.0078	0.0072
19	0.0027	0.0016	0.0019	0.0036	0.0032	0.0041	0.0057	0.0056
20	0.0027	0.0016	0.0013	0.0036	0.0032	0.0028	0.0021	0.0056
21	0.0027	0.0016	0.0013	0.0030	0.0019	0.0021	0.0021	0.0032
22	0.0027	0.0016	0.0013	0.0024	0.0019	0.0021	0.0007	0.0032
23	0.0027	0.0016	0.0006	0.0012	0.0013	0.0014	0.0007	0.0024
24	0.0027	0.0008	0.0006	0.0012	0.0013	0.0000	0.0007	0.0024
25	0.0027	0.0008	0.0006	0.0012	0.0013	0.0000	0.0007	0.0016
26	0.0027	0.0000	0.0006	0.0012	0.0013	0.0000	0.0007	0.0016
27	0.0027	0.0000	0.0006	0.0006	0.0013	0.0000	0.0007	0.0008
28	0.0027	0.0000	0.0006	0.0006	0.0013	0.0000	0.0007	0.0008
29	0.0027	0.0000	0.0006	0.0006	0.0013	0.0000	0.0007	0.0008
30	0.0014	0.0000	0.0000	0.0006	0.0006	0.0000	0.0007	0.0008
31	0.0014	0.0000	0.0000	0.0006	0.0000	0.0000	0.0007	0.0008
32	0.0014	0.0000	0.0000	0.0006	0.0000	0.0000	0.0007	0.0000
33	0.0014	0.0000	0.0000	0.0006	0.0000	0.0000	0.0000	0.0000
34	0.0000	0.0000	0.0000	0.0006	0.0000	0.0000	0.0000	0.0000
35	0.0000	0.0000	0.0000	0.0006	0.0000	0.0000	0.0000	0.0000
36	0.0000	0.0000	0.0000	0.0000	0.0000	0.0000	0.0000	0.0000

31
Table 10: CCDF of TV LOS part 2. Each column is the CCDF of LOS for patients entered in time period of column index, e.g. column 1 is the CCDF of LOS for patients entered in 00:00-01:00 (Use data set 4.)

	17	18	19	20	21	22	23	24
0	0.9289	0.9505	0.9503	0.9602	0.9548	0.9480	0.9609	0.8093
1	0.8340	0.8405	0.8460	0.8673	0.8312	0.8400	0.6960	0.7089
2	0.6774	0.6961	0.7074	0.6948	0.6704	0.5695	0.5161	0.4961
3	0.4809	0.5189	0.4939	0.5098	0.3502	0.3834	0.3490	0.3385
4	0.3285	0.3291	0.3472	0.2600	0.2195	0.2380	0.2434	0.2679
5	0.2312	0.2309	0.1573	0.1702	0.1355	0.1755	0.1975	0.2249
6	0.1643	0.1058	0.1051	0.1132	0.1014	0.1511	0.1779	0.1996
7	0.0728	0.0781	0.0725	0.0890	0.0872	0.1348	0.1496	0.1797
8	0.0550	0.0579	0.0481	0.0765	0.0777	0.1162	0.1447	0.1411
9	0.0398	0.0462	0.0432	0.0679	0.0721	0.1040	0.1065	0.1080
10	0.0305	0.0395	0.0375	0.0640	0.0658	0.0877	0.0860	0.0838
11	0.0246	0.0378	0.0342	0.0585	0.0531	0.0674	0.0596	0.0595
12	0.0229	0.0361	0.0310	0.0484	0.0420	0.0479	0.0371	0.0408
13	0.0195	0.0327	0.0261	0.0328	0.0341	0.0325	0.0254	0.0254
14	0.0178	0.0285	0.0171	0.0273	0.0198	0.0195	0.0176	0.0143
15	0.0144	0.0227	0.0139	0.0219	0.0151	0.0114	0.0127	0.0110
16	0.0127	0.0168	0.0098	0.0133	0.0087	0.0065	0.0078	0.0088
17	0.0093	0.0118	0.0065	0.0094	0.0024	0.0024	0.0029	0.0044
18	0.0076	0.0109	0.0041	0.0055	0.0016	0.0016	0.0029	0.0044
19	0.0051	0.0050	0.0024	0.0031	0.0016	0.0016	0.0020	0.0033
20	0.0034	0.0025	0.0016	0.0000	0.0008	0.0016	0.0020	0.0033
21	0.0017	0.0025	0.0016	0.0000	0.0008	0.0000	0.0020	0.0033
22	0.0008	0.0025	0.0008	0.0000	0.0008	0.0000	0.0020	0.0033
23	0.0000	0.0017	0.0000	0.0000	0.0008	0.0000	0.0010	0.0033
24	0.0000	0.0017	0.0000	0.0000	0.0008	0.0000	0.0000	0.0011
25	0.0000	0.0017	0.0000	0.0000	0.0008	0.0000	0.0000	0.0011
26	0.0000	0.0008	0.0000	0.0000	0.0000	0.0000	0.0000	0.0011
27	0.0000	0.0000	0.0000	0.0000	0.0000	0.0000	0.0000	0.0011
28	0.0000	0.0000	0.0000	0.0000	0.0000	0.0000	0.0000	0.0011
29	0.0000	0.0000	0.0000	0.0000	0.0000	0.0000	0.0000	0.0011
30	0.0000	0.0000	0.0000	0.0000	0.0000	0.0000	0.0000	0.0011
31	0.0000	0.0000	0.0000	0.0000	0.0000	0.0000	0.0000	0.0011
32	0.0000	0.0000	0.0000	0.0000	0.0000	0.0000	0.0000	0.0011
33	0.0000	0.0000	0.0000	0.0000	0.0000	0.0000	0.0000	0.0011
34	0.0000	0.0000	0.0000	0.0000	0.0000	0.0000	0.0000	0.0011
35	0.0000	0.0000	0.0000	0.0000	0.0000	0.0000	0.0000	0.0011
36	0.0000	0.0000	0.0000	0.0000	0.0000	0.0000	0.0000	0.0000

32
Table 11: CCDF of TV LOS part 3. Each column is the CCDF of LOS for patients entered in time period of column index, e.g. column 1 is the CCDF of LOS for patients entered in 00:00-01:00 (Use data set 4.)

5. Departure process

In this section, we explore the departure process of the queueing system. Under the $M_t/GI_t/\infty$ model setting, the departure process is also a non-homogeneous Poisson process, thus it is of interest to see what the departure process looks like. The main idea is that we consider the process in reversed time and view the departure process as "arrival process". Then we can do a similar analysis as in Section 3.

5.1. Daily total departures

Paralleling §3 of the main paper, we start by looking at the daily total departures. Here we consider the departure process and accordingly the population changes a little bit compared to the previous sections. In this section, we consider the patients we exited the ED (the EIMU) from Dec. 5, 2004 to May 28, 2005, which is 23,407 patients in total. We will do everything in reverse-time if not specified.

Table 12 shows the number of daily total departures of the 25 weeks in reversed time. This table is similar to the daily total arrivals in Table 2 of the main paper. The mean of each week is almost the same as for the arrivals. The mean of each day of week also looks like the arrivals. The difference is in the variance of the daily totals of each day of week. The variance of departures is relatively higher than the arrivals.

Again, we fit the Gaussian model for the departures:

$$T(w, d) = A + Bw + Cd + G(0, \sigma^2), \quad (3)$$

where the parameters have the same meaning as before. We have the ANOVA table for this regression in Table 13. We see that, again, both the Week factor and the Day of Week factor are significant and the DoW factor explains most of the variance. The mean sum of square for the residuals is $\hat{\sigma}^2 = 202.5 = 14.23^2$, which is higher than that of the arrival process. The variance-to-mean ratio is $202.5/133.8 = 1.51$.

If we omit the Week factor and consider the single-factor model, then the mean sum of square for the residuals is $(10661 + 29156)/(24 + 144) = 237.0$, and the variance-to-mean ratio is $237.0/133.8 = 1.77$. The estimated coefficients for the single-factor model is shown in Table 14, and a histogram of residuals and a Q-Q plot for the studentized residuals are shown in Figure 21, which is parallel to Figure 2 of the main paper. From the residuals we see that the Gaussian model works well for the departure process in reversed time.

	Sat.	Fri.	Thu.	Wed.	Tue.	Mon.	Sun.	Total	Mean
25	97	130	155	142	151	147	156	978	139.71
24	86	125	147	159	141	180	143	981	140.14
23	94	130	98	128	160	136	144	890	127.14
22	104	115	109	114	148	147	142	879	125.57
21	109	112	137	128	165	163	126	940	134.29
20	108	99	117	135	128	160	155	902	128.86
19	117	108	125	151	151	135	130	917	131.00
18	105	125	130	153	152	136	162	963	137.57
17	129	118	133	121	168	124	151	944	134.86
16	113	88	139	137	185	160	151	973	139.00
15	103	124	160	154	131	148	180	1000	142.86
14	95	142	133	153	150	157	158	988	141.14
13	109	113	144	124	180	163	167	1000	142.86
12	91	129	123	137	144	153	156	933	133.29
11	124	135	134	143	120	125	151	932	133.14
10	79	83	100	116	122	128	131	759	108.43
9	85	79	140	141	127	157	169	898	128.29
8	108	122	120	148	161	137	171	967	138.14
7	110	112	135	105	157	163	167	949	135.57
6	102	122	159	136	161	131	182	993	141.86
5	99	115	149	136	162	168	172	1001	143.00
4	112	99	119	139	145	174	154	942	134.57
3	91	118	128	148	141	164	152	942	134.57
2	90	123	115	141	141	123	144	877	125.29
1	102	100	121	114	127	145	150	859	122.71
Total	2562	2866	3270	3403	3718	3724	3864	23407	
Mean	102.48	114.64	130.8	136.12	148.72	148.96	154.56	936.28	
Var.	146.18	253.74	276.00	204.86	294.54	270.46	213.26	3109.46	

Table 12: Number of departures at EIMU of each day from Dec. 5, 2004 to May 28, 2005 (25 weeks).

5.2. Departure Pattern Within Days

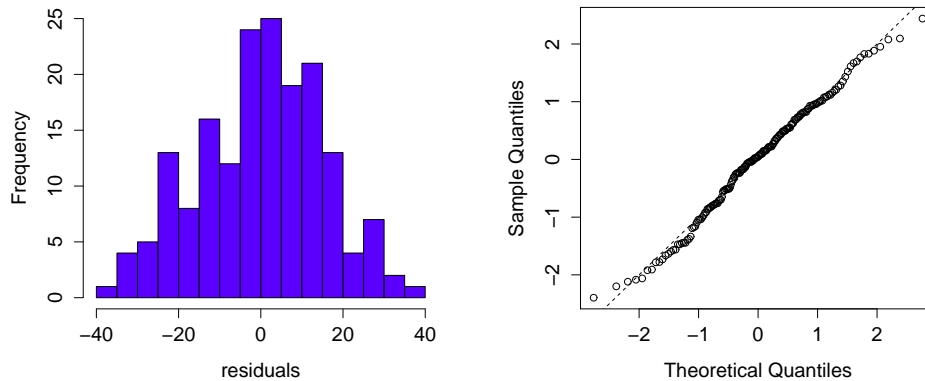
Now we turn to the time structure of departure rate within days. Figure 22 shows the estimated departure rate function over a week in the reverse-time view. We see that the rate has midnight surges clearly and the peaks

Factor	Sum of square	df	Mean sum of square	F statistics	P-values
Week	10661	24	444.2	2.19	<0.01
DoW	56146	6	9357.6	46.22	<0.01
Residuals	29156	144	202.5		

Table 13: ANOVA table for Gaussian model for the daily total departures. (Use data set 7.)

Coeffitients	Estimate	SE
A	133.754	3.079
C.Sun	20.806	4.354
C.Mon	15.206	4.354
C.Tue	14.966	4.354
C.Wed	2.366	4.354
C.Thu	-2.954	4.354
C.Fri	-19.114	4.354
C.Sat	-31.274	4.354

Table 14: Regression result for daily total model with only DoW factor for the departures. (We set $\sum C = 0$). (Use data set 7.)



(a) Histogram of residuals.

(b) Q-Q plot for studentized residuals.

Figure 21: Residuals of regression of daily total departures with only DoW factor. (Use data set 7.)

are increasing. This may correspond to the number of daily total arrivals for each day of week. The departure rate is relatively stable from the afternoon to the midnight.

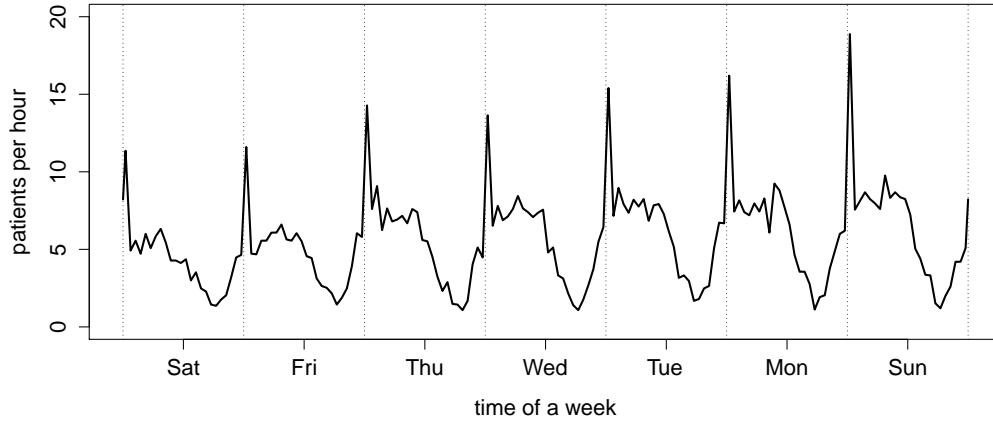


Figure 22: Average departure rate for EIMU by reversed time. (Use data set 7.)

As for arrivals, we divided the patients into two groups according to the admission decision in the previous sections. Parallel to Figure 14, 15 and 16, we plot Figure 23, 24 and 25. From these 3 plots, we see that the departure rate of non-admitted patients is almost always higher than the rate of admitted patients and the proportion of admitted patients is extremely low at 7-8 a.m. of each day. The proportion of admission in reversed departure process is less regular than the one of arrival process.

5.3. The LoS Seen By Departures

We have seen that the LoS depends strong on the arrival time in §4.3 of the main paper. We want to see whether that is also the case for the reversed process.

Figure 26(a) shows that the LoS the distribution also depends on the departure time. Interestingly, the LoS is long in the morning, which means patients who left the emergency department in the morning experienced a long LoS. As a consequence, those patients arrived in the ED in the late evening. This is reasonable, because these patients might have to wait to the

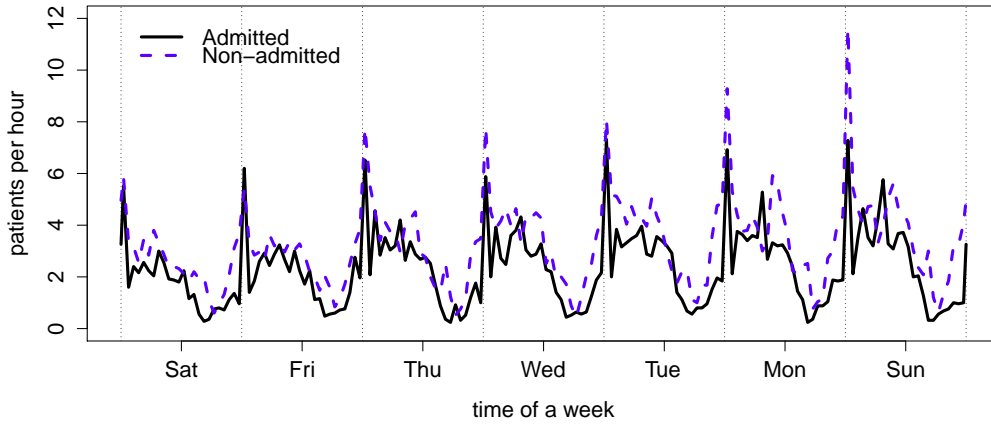


Figure 23: Departure rates for the admitted and non-admitted patients in reversed time. (Use data set 8 and 9.)

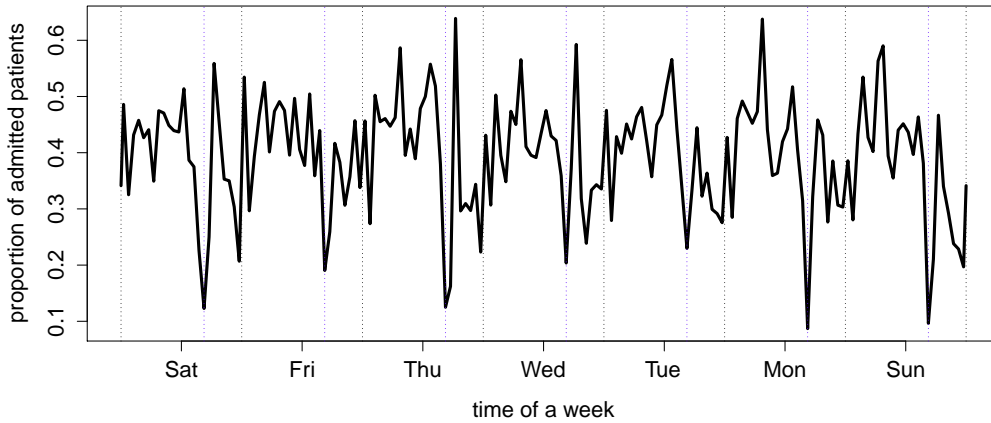


Figure 24: Estimated proportion of admitted patients in reversed departure process of EIMU for a week. The dotted blue lines are 7 a.m. to 8 a.m.. (Use data set 8 and 9.)

morning to see an appropriate doctor before an admission decision can be made.

We now turn to the two groups of patients, admitted and non-admitted.

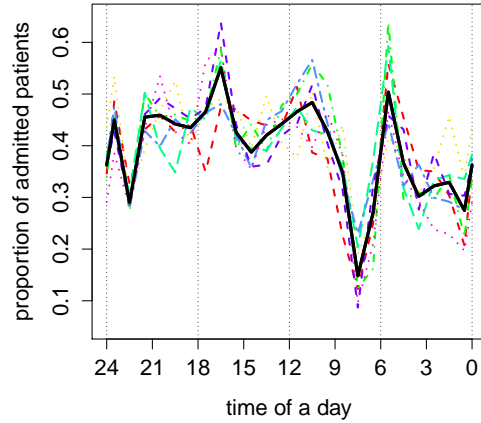
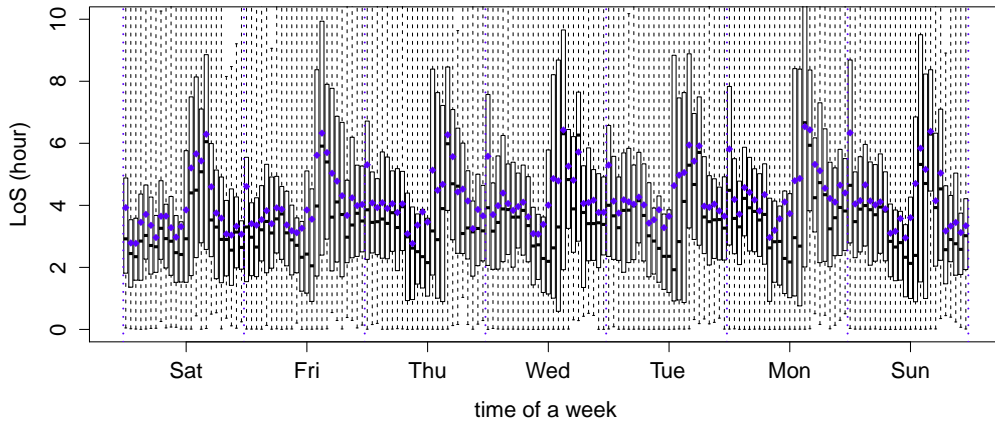
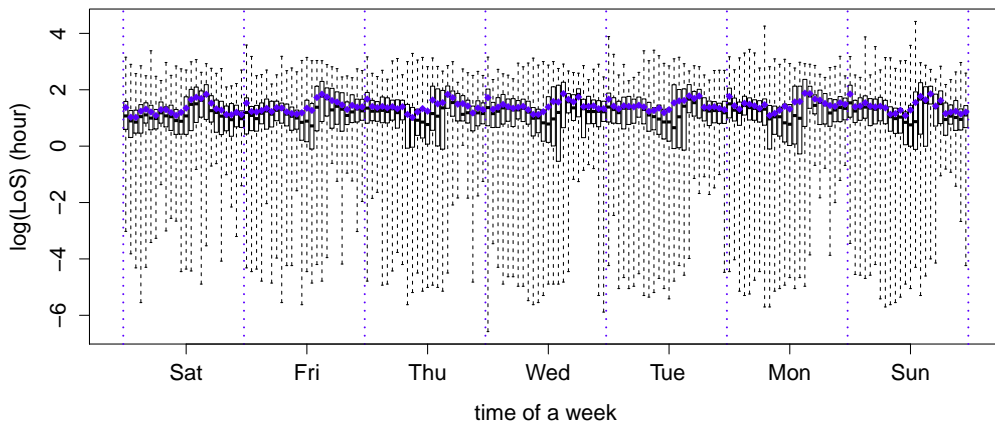


Figure 25: Estimated proportion of admitted patients in arrival process of EIMU for a day combining all days together (black solid line) and the proportions of admitted patients for each day of week. (Use data set 8 and 9.)

Figure 27 is analogous to Figure 11 in the main paper. We see that the midnight surge is caused by the non-admitted patients, and the non-admitted patients are more influenced by time of the day. The mean of the LoS is almost constant for the admitted patients from 4 p.m. to 3 a.m. At 5 a.m. the mean is quite large and after that it slowly decreases until 2 p.m. The one for the non-admitted patients has a obvious ridge in the morning.

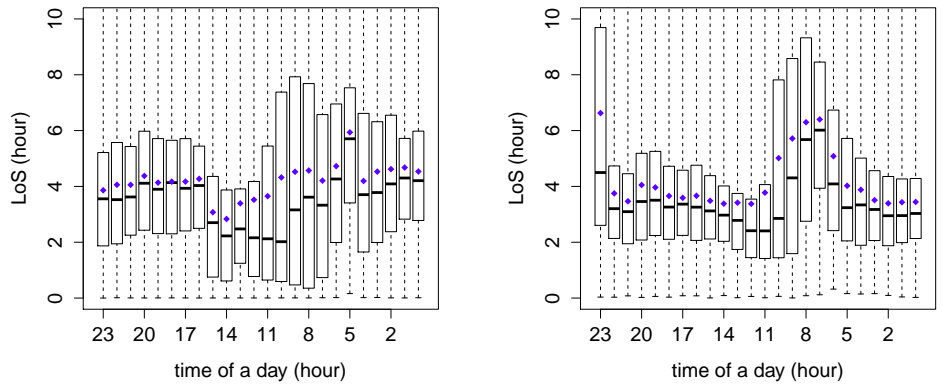


(a) LoS by time.



(b) $\log(\text{LoS})$ by time.

Figure 26: Time view of LOS in reverse time. The blue dots are means and the black bars are medians. (Use data set 7.)



(a) LoS of Admitted patients by reversed time. (b) LoS of non-admitted patients by reversed time.

Figure 27: Time view of LoS for the 2 groups. (Use data set 8 and 9.)

6. Comparison with Simulation

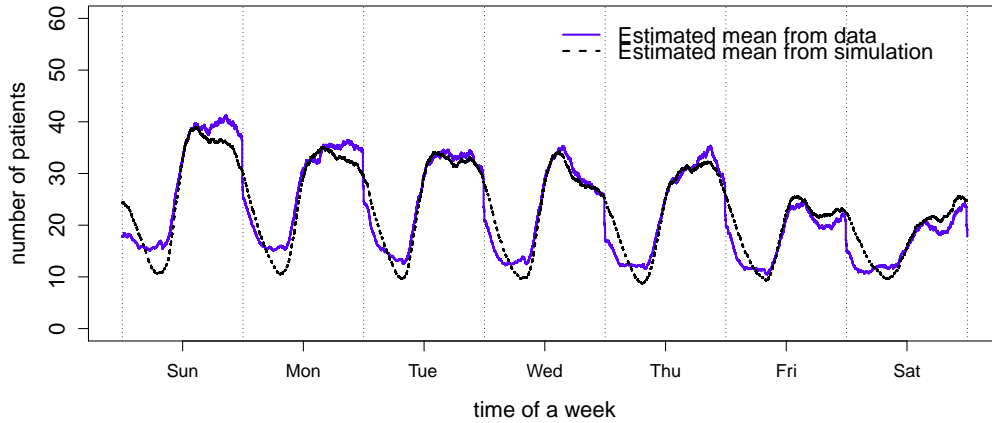
6.1. Simulation for the model

We conducted six different simulations to see if our model can characterize the ED well. They are done as following:

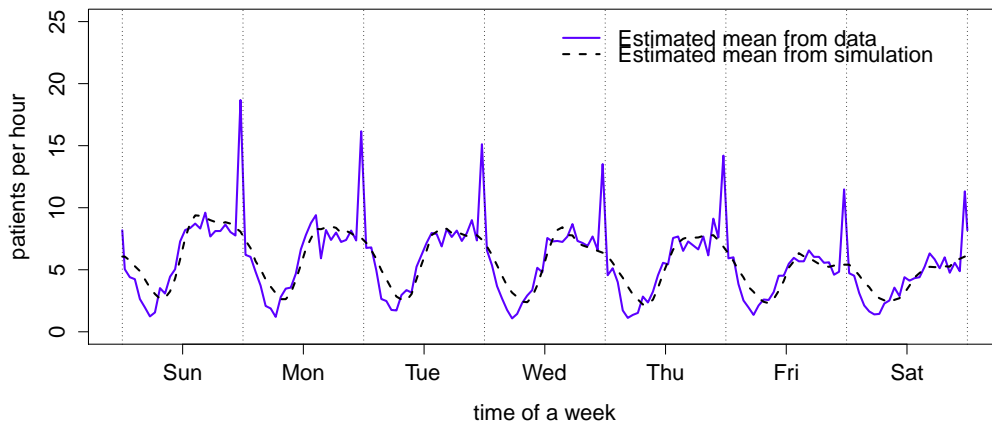
- A: We use the original arrival data and the non-time-varying LoS; i.e., we estimated the LoS by combining all the data for each group.
- B: We use the original arrival data and the time-varying LoS in a day view; i.e., we estimated the distribution of LoS hourly for every hour of a day and assume a periodic structure for the LoS of period length 24 hours.
- C: We use the original arrival data and the time-varying LoS in a week view; i.e., we estimated the distribution of LoS hourly for every hour of a week and assume a periodic structure for the LoS of period length 1 week.
- A': We treat the arrival process as an NHPP given daily total arrivals, and the non-time-varying LoS.
- B': We treat the arrival process as an NHPP given daily total arrivals, and the time-varying LoS in a day view.
- C': We treat the arrival process as an NHPP given daily total arrivals, and the time-varying LoS in a week view.

The size of each simulation is 1000 (For simulation A,B and C using original arrival data, we repeated the 25 weeks for 40 times so that we have in total 1000 weeks). We compute the averaged number of patients in the system and the averaged departure rate using the simulation results and compared them to the one that estimated from the raw data. We show these, respectively, in Figures 28, 29, 30, 31, 32 and 33.

These simulation results are informative. From simulation A we see that a model with non-time-varying does not work for the system. It cannot capture the midnight surge even we use the original arrival data. The result of simulation B is better than A, but still not good enough. It captures the midnight surge, but there is an obvious gap between the curves of number in the system. For Sunday and Monday, the simulated one is lower than the



(a) Number of patients in system.

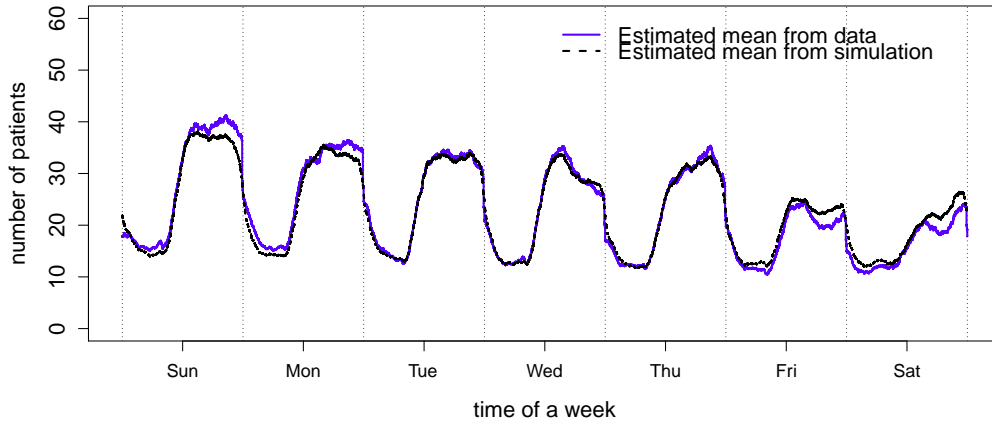


(b) Departure rate.

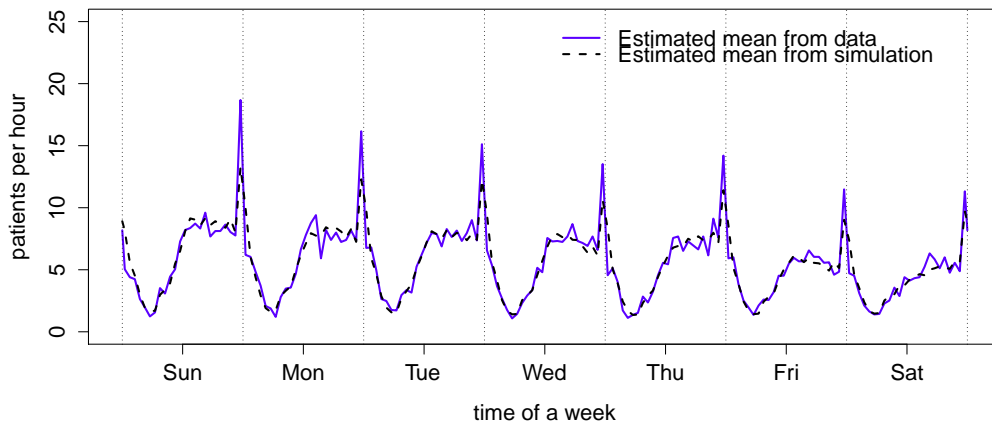
Figure 28: Result of simulation A

real one while for Friday and Saturday the simulated one is higher than the real one. For simulation C, the curves almost perfectly coincide.

Simulation A', B' and C' look almost the same as A, B and C respectively. The result for simulation C', which is the model we propose, looks good. These simulation results indicate that our model for the arrival process works



(a) Number of patients in system.

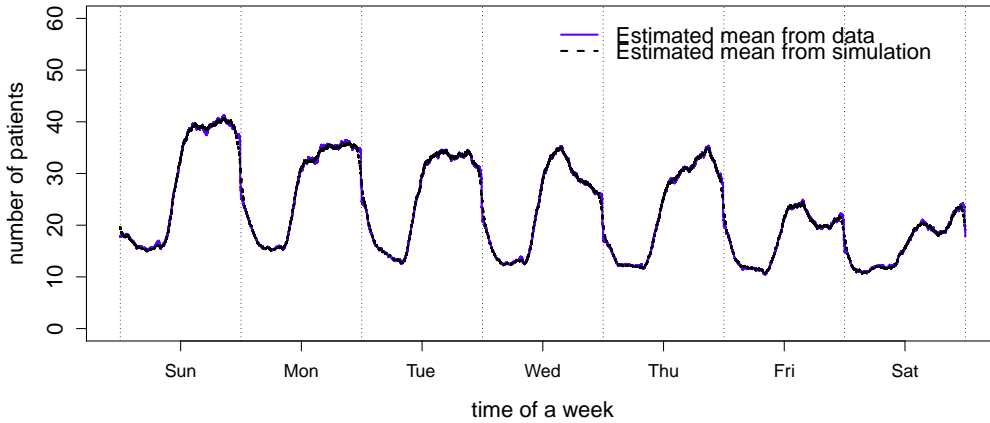


(b) Departure rate.

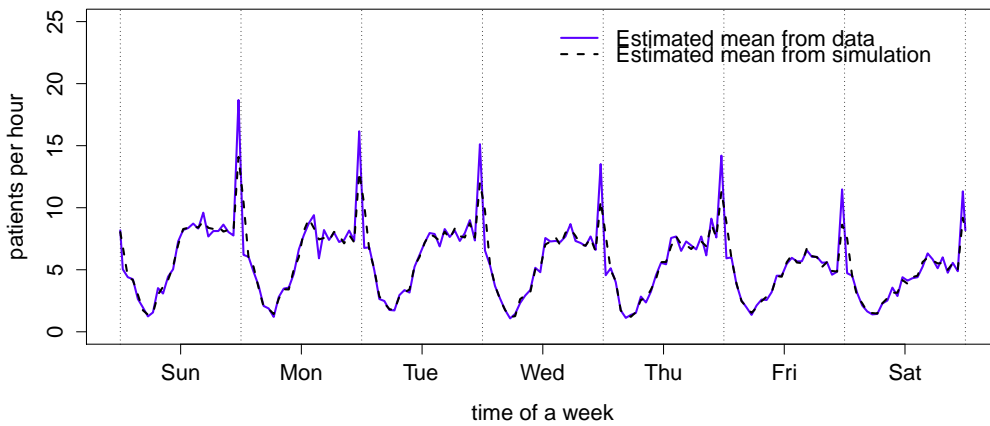
Figure 29: Result of simulation B

well.

In Figure 34 we compute the variance of number of patients hourly for each hour in a week. We see that the variance estimated from the data is higher than the one estimated from the simulation C' in the day time.



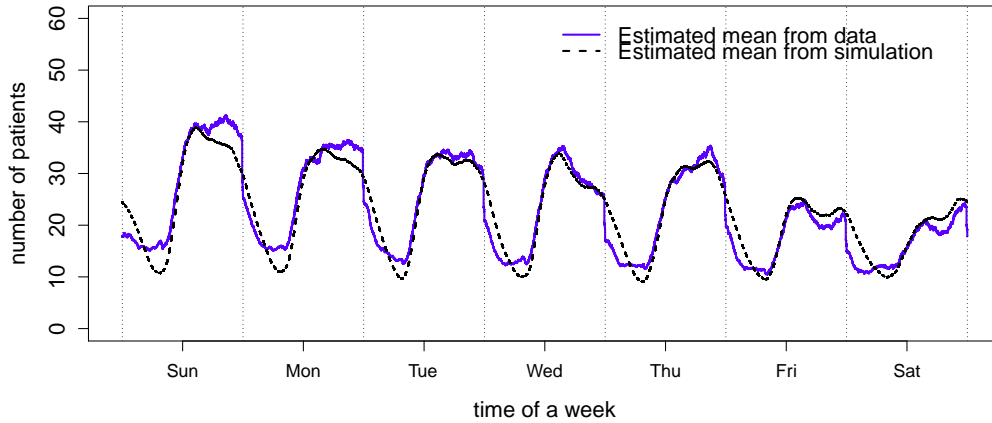
(a) Number of patients in system.



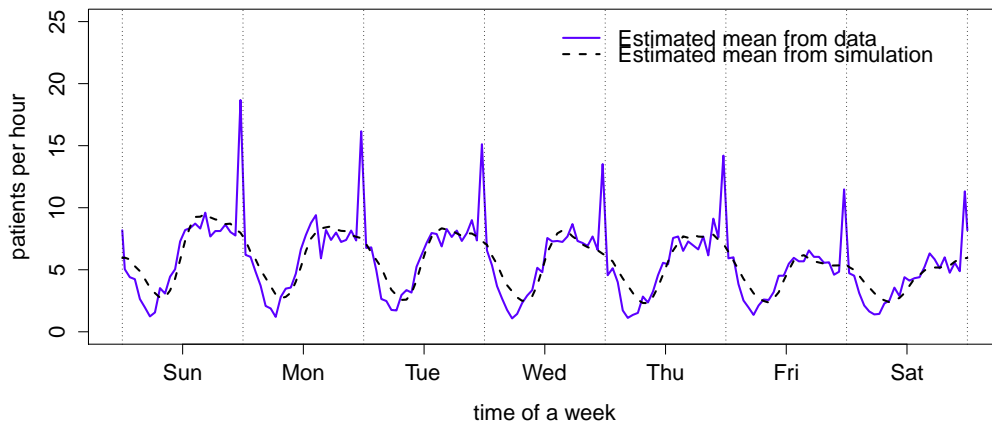
(b) Departure rate.

Figure 30: Result of simulation C

We also noticed that in all the simulation we underestimated the midnight surge effect, this may due to the resolution of our model. The midnight surge occurs in a single hour, but we estimated both the arrival rate and the distribution of LoS hourly, so in some sense we averaged everything in a hour. We know estimated the arrival rate hourly and then got the rate



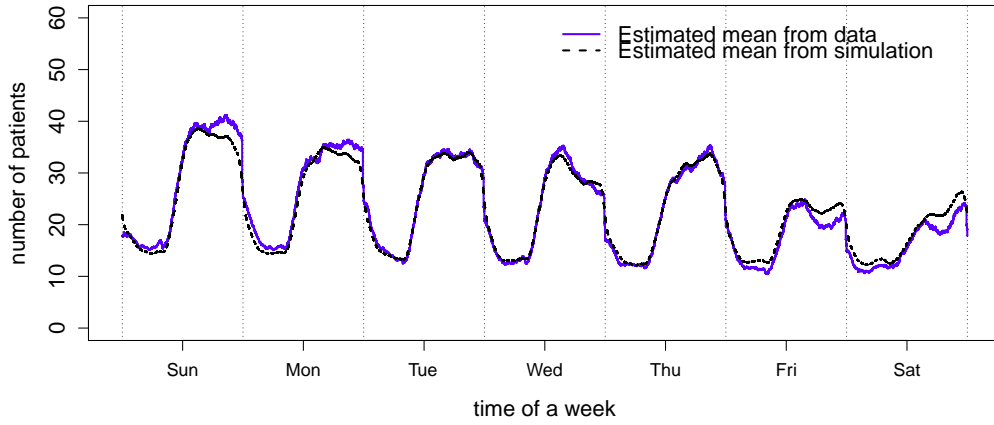
(a) Number of patients in system.



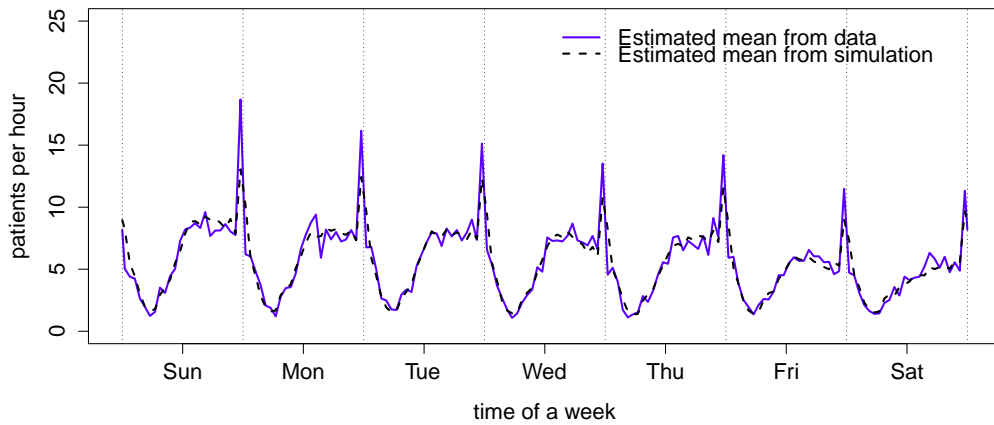
(b) Departure rate.

Figure 31: Result of simulation A'

function by linear interpolation may cause some errors compared to keep the rate constant in each hour, but this will make the rate changing continuously, which we think more close to the reality.

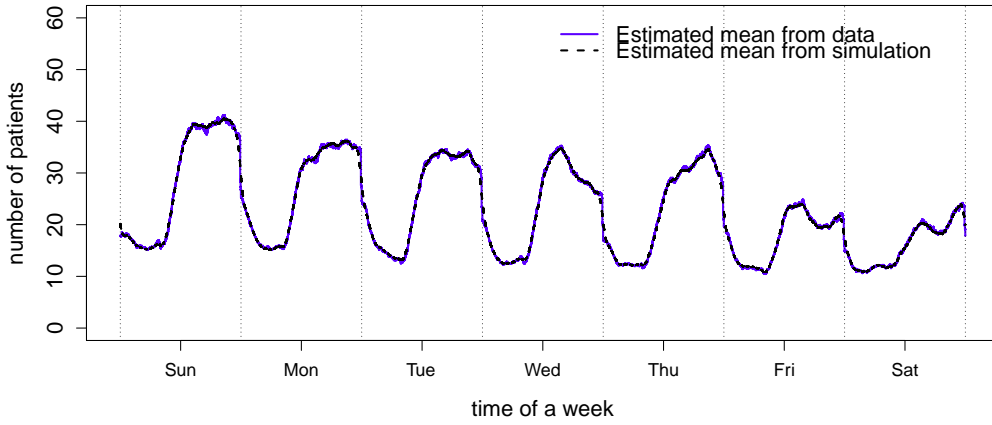


(a) Number of patients in system.

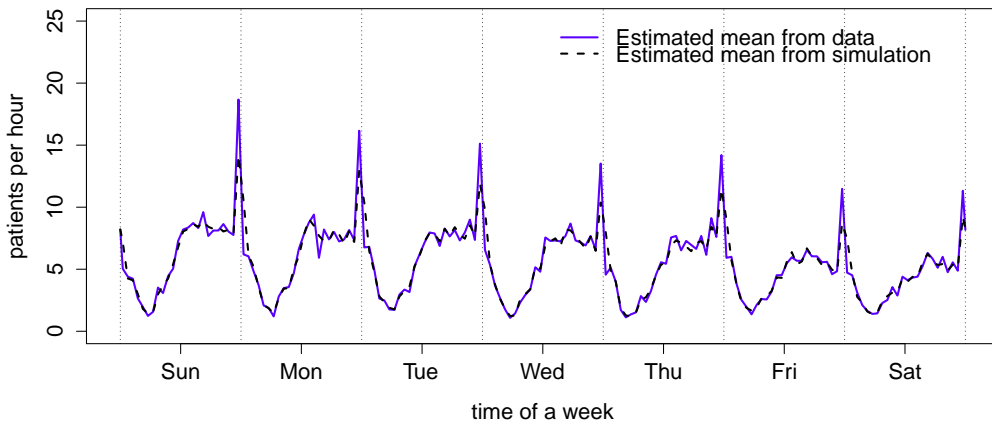


(b) Departure rate.

Figure 32: Result of simulation B'



(a) Number of patients in system.



(b) Departure rate.

Figure 33: Result of simulation C'

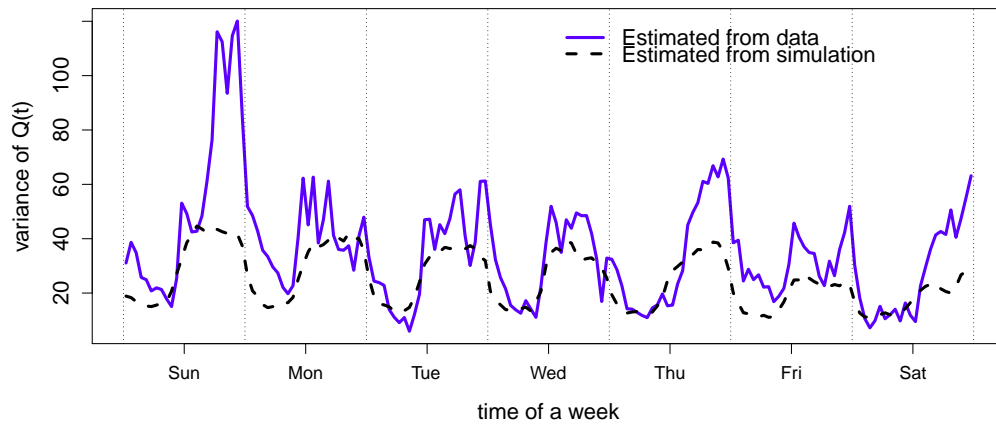


Figure 34: Variance of the number of patients in the system estimated from the data and simulation C^2 .

7. Occupancy and Time-Varying Little's Law

This is the first section not in the main paper. This section is devoted to developing a discrete-time version of the time-varying Little's law (TVLL), which is natural using the X matrix introduced in §4.2 of the main paper. More on the TVLL will appear in [5].

The TVLL is established by Bertsimas and Mourtzinou [2]. Under very general regularity conditions [2, 3], we have

$$\mathbb{E}(L(t)) = \int_{-\infty}^t G_s^c(t-s)\lambda(s)ds, \quad (4)$$

where $\lambda(s)$ is arrival rate function, $W(t)$ is the waiting time of the last customer to arrive at or before time t so $G_t(x) = P(W(t) \leq x | \mathcal{A}_t)$, $x \geq 0$, is the conditional cumulative distribution function of the waiting time for a new arrival at time t , and

$$L(t) = \int_{-\infty}^t I_{W(s) > t-s} dA(s) \quad (5)$$

is the number in the system at time t .

The relationship between the TVLL and infinite-server (IS) queueing system, especially for $M_t/GI_t/\infty$ model, is discussed in [4]. It points out that the TVLL can be regarded as part of the theory of IS models since it can be regarded as a general IS model if we simply call the waiting time the service time in the IS model. In our case, we think the LoS is the service time.

The discrete-time TVLL is much easier to understand. In this section, we want to show that the discrete version of TVLL is essentially a counting problem. Let $X_{k,j}$ be the number of arrivals in discrete time period k that have a LoS of j time periods, $j \geq 0$. Then

$$A_k = \sum_{j=0}^{\infty} X_{k,j} \quad \text{and} \quad D_k = \sum_{j=0}^{\infty} X_{k-j,j} \quad (6)$$

are the number of arrivals and departures of discrete time period k .

Next, let

$$Y_{k,j} = \sum_{i=j+1}^{\infty} X_{k,i}$$

be the number of arrivals in discrete time period k that have a LoS strictly greater than j . Then

$$Q_k = \sum_{j=0}^{\infty} Y_{k-j,j} = \sum_{j=0}^{\infty} A_{k-j} \frac{Y_{k-j,j}}{A_{k-j}} \quad (7)$$

is the number in system at the end of discrete time period k . Further, if we let

$$\bar{F}_{k,j}^c = \frac{Y_{k,j}}{A_k} \quad (8)$$

be the proportion of all arrivals at time k that depart strictly later than time $k + j$, for $j \geq 0$. Then $\bar{F}_{k-j,j}^c$ is the proportion of arrivals at time $k - j$ that depart after time k . Then (7) becomes

$$Q_k = \sum_{j=0}^{\infty} Y_{k-j,j} = \sum_{j=0}^{\infty} A_{k-j} \bar{F}_{k-j,j}^c. \quad (9)$$

Noting that if the length of discrete time periods go to 0, (9) is equivalent to (5).

Now we assume that $Q_0 = 0$ (We may be able to regard all customers initially in the system as arrivals at time 0.) and we can rewrite (9) as

$$Q_k = \sum_{j=0}^k Y_{j,k-j} = \sum_{j=0}^k A_j \bar{F}_{j,k-j}^c. \quad (10)$$

Additionally, we assume a periodic structure over successive periods of d discrete times. We assume that we have sufficient data to estimate averages over n periods, containing nd time periods. We also assume that $X_{k,j} = 0$ for $j \geq d$, so that $Y_{k,j} = 0$ for $j \geq d - 1$.

In this periodic settings, we construct averages. We have

$$\begin{aligned} \bar{X}_{k-j,j} &= \frac{1}{n} \sum_{m=1}^n X_{(m-1)d+k-j,j}, & \bar{A}_k &= \frac{1}{n} \sum_{m=1}^n A_{(m-1)d+k} \\ \text{and } \bar{D}_k &= \frac{1}{n} \sum_{m=1}^n D_{(m-1)d+k}, \end{aligned} \quad (11)$$

for $0 \leq k < d$ and positive integers n , m and d . For example, we might have $d = 24$ for the number of hours over a day or $d = 7 * 24 = 168$ for a week.

Also we construct averages for Q_k and $Y_{k-j,j}$ by letting

$$\bar{Y}_{k-j,j} = \frac{1}{n} \sum_{m=1}^n Y_{(m-1)d+k-j,j}, \quad \text{and} \quad \bar{Q}_k = \frac{1}{n} \sum_{m=1}^n Q_{(m-1)d+k}, \quad (12)$$

for $0 \leq k < d$, $0 \leq j < d-1$ and define $\bar{Y}_{k-j,j} \equiv \bar{Y}_{d+k-j,j}$ for $k-j < 0$. Then we get

$$\begin{aligned} \bar{Q}_k &= \frac{1}{n} \sum_{m=1}^n Q_{(m-1)d+k} \\ &= \frac{1}{n} \sum_{m=1}^n \sum_{j=0}^{d-1} Y_{(m-1)d+k-j,j} \\ &= \sum_{j=0}^{d-1} \frac{1}{n} \sum_{m=1}^n Y_{(m-1)d+k-j,j} \\ &= \sum_{j=0}^{d-1} \bar{Y}_{k-j,j} \\ &= \sum_{j=0}^{d-1} \bar{A}_{k-j} \bar{F}_{k-j,j}^{c,*}, \end{aligned} \quad (13)$$

where

$$\bar{F}_{k-j,j}^{c,*} = \frac{\bar{Y}_{k-j,j}}{\bar{A}_{k-j}} = \frac{\sum_{m=1}^n Y_{(m-1)d+k-j,j}}{\sum_{m=1}^n A_{(m-1)d+k-j}}. \quad (14)$$

We recognize that (13) is a discrete empirical analog of the TVLL, expressed as

$$\mathbb{E}(Q(t)) = \int_0^t P(W(s) > t-s) \lambda(s) ds. \quad (15)$$

8. Fitting a Stationary Birth-and-Death Process to the Data

In [6] we introduced a new “grey-box” stochastic modeling approach. In particular, we proposed approaching a queueing application where we do not know what model is appropriate by fitting a stationary BD process to an observed segment of the sample path of a queue-length stochastic process estimated from system data, assuming only that the queue length increases

and decreases in unit steps. Just as is commonly done for estimating rates in a BD process [18, 19, 20], we estimate the birth rate in state k from arrival data over an interval $[0, t]$ by $\bar{\lambda}_k \equiv \bar{\lambda}_k(t)$, the number of arrivals observed in that state, divided by the total time spent on that state, while we estimate the death rate in state k by $\bar{\mu}_k \equiv \bar{\mu}_k(t)$, the number of departures observed in that state, divided by the total time spent on that state. As usual, the steady-state distribution of that fitted BD model, denoted by $\bar{\alpha}_k^e \equiv \bar{\alpha}_k^e(t)$ (with superscript e indicating the estimated rates), is well defined (under regularity conditions, see [8]) and is characterized as the unique probability vector satisfying the local balance equations,

$$\bar{\alpha}_k^e \bar{\lambda}_k = \bar{\alpha}_{k+1}^e \bar{\mu}_{k+1}, \quad k \geq 0. \quad (16)$$

(We assume that limiting values of the rates as $t \rightarrow \infty$ exist and that our estimators are consistent, so we omit the t .)

The BD process is appealing as a grey-box model for queueing systems, because the fitted BD steady-state distribution $\{\bar{\alpha}_k^e : k \geq 0\}$ in (16) closely matches the empirical steady-state distribution, $\{\bar{\alpha}_k : k \geq 0\}$, where $\bar{\alpha}_k \equiv \bar{\alpha}_k(t)$ is the proportion of total time spent in each state. Indeed, as has been known for some time (e.g., see Chapter 4 of [21]), under regularity conditions, these two distributions coincide asymptotically as t (and thus the sample size) increases, even if the actual system evolves in a very different way from the fitted BD process. For example, the actual process $\{Q(t) : t \geq 0\}$ might be periodic or non-Markovian.

If we directly fit a BD process to data as just described, we should not conclude without further testing that the underlying queue-length process actually is a BD process. In fact, the main point of [8] was to caution against drawing unwarranted positive conclusions from a close similarity in the steady-state distributions, because these two distributions are automatically closely related. Nevertheless, the fitted BD process can provide useful insight about the underlying system.

The first paper [6] investigated fitting BD processes to the queue length processes of various $GI/GI/s$ queues, and investigated what can be learned about the underlying model. The second paper [7] investigated fitting BD processes to the queue length processes of various $M_t/GI/s$ queues having periodic arrival rate functions, and again investigated what can be learned about the underlying model. In both cases we found that these models have “signatures” that can be recognized in the fitted virth and death rates.

In fact, our earlier paper [8] was largely motivated by exploratory data analysis carried out in an earlier 2011 version of §3 of [14]. They had fit several candidate models to data on the number of patients in a hospital emergency department, and found that a BD process fit better than others. After writing [8], cautioning against drawing unwarranted positive conclusions, we realized that fitting BD processes to data might indeed be useful, and started the investigation in [6]. While the discussion in [14] changed significantly since the earlier version, the issue here is still discussed in §3.2.3 of [14] on “state dependency.”

First, we look at the empirical steady-state distributions from the ED data and the fitted BD process as before. To make these two steady state distributions identical, we make the initial state the same as the end state; see [8]. Here we make the initial and final states be times when the number of patients in the ED is 26. Figure 35 empirically confirms the theoretical result from [8]. Figure 35 is very similar to Figure 4 in [14].

The distribution is in Figure 35 and the fitted birth and death rates in Figure 36. Next, the fitted birth and death rates are shown in Figure 36.

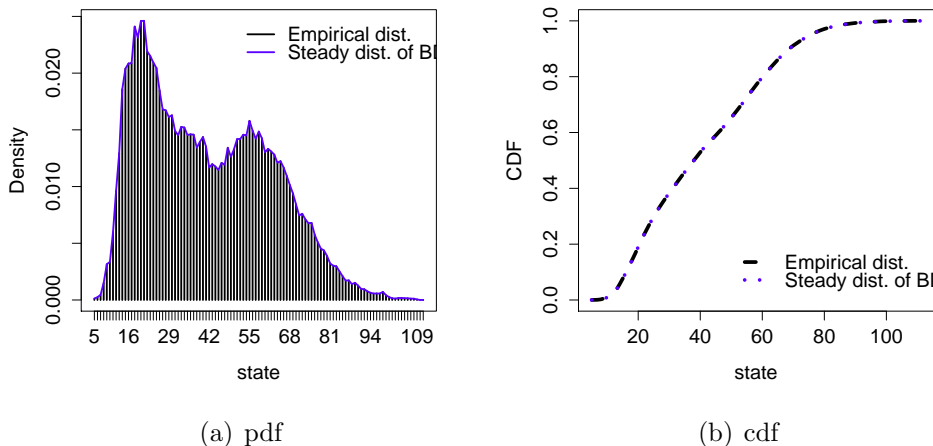
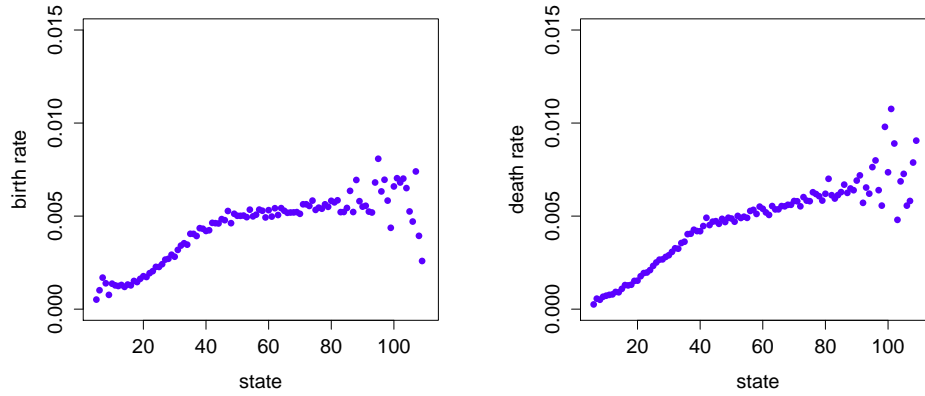


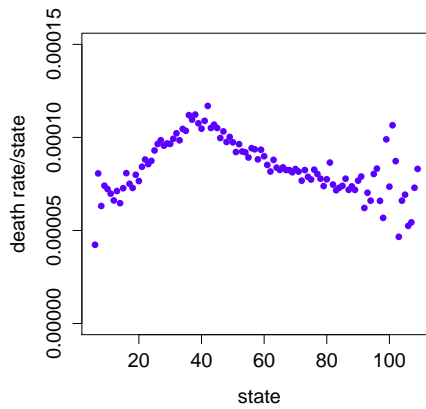
Figure 35: Empirical and BD fitted steady state distribution of the patient flow in ED.

Clearly we can see a change of slope in the estimated death rates at state 40, which coincide with the number of beds in the ED. However, if the system actually were a 40-server queueing system, with iid service times, then the death rates should be a horizontal line for states large than 40, as



(a) Birth rate

(b) Death rate



(c) Death rate/State

Figure 36: Estimated birth and death rates and death rates per patient of the BD process of ED.

illustrated by [6, 7]. However, as discussed in §3.1 of [14], the capacity of the ED is actually quite flexible, so that we should not expect it to perform as simply as a queueing model with the fixed number of 40 servers. Consistent with that flexibility, we see that the death rate is increasing when there are more than 40 patients. Just as in [14], we also show the estimated death (service) rate per patient. Our examination of this state dependency confirms conclusions reached in [14]. In §3.2.3 they suggested four possible reasons,

but they did not point out the relationship between the turning point and the number of servers.

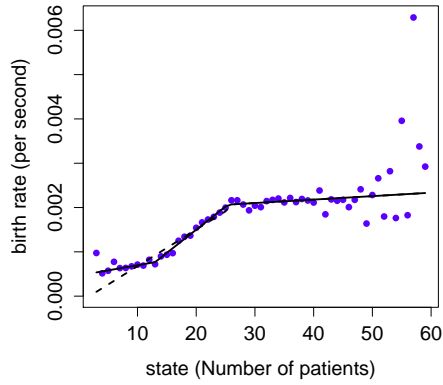
The birth rates also tend to become horizontal when there are more than about 45-50 patients, a reason may be new patients were sent to other hospitals when this one is full. For further discussion of this example, see §6.3 of [7], which also observes that the fitted birth rates are consistent with the periodic time-varying arrival rate function, which we know holds for the ED.

Given the shape of the birth and death rates, we try to fit linear functions to the rates. We fit piecewise linear models to the birth and death rates. We tried two ways for the birth rate: one is fitting it with 2 pieces of lines and the other is with 3 pieces of lines. We show the fitting in Figure 37 and put the estimated parameters in Table 15. The comparison between the steady state distribution by the fitted birth and death models and the empirical distribution is shown in Figure 38.

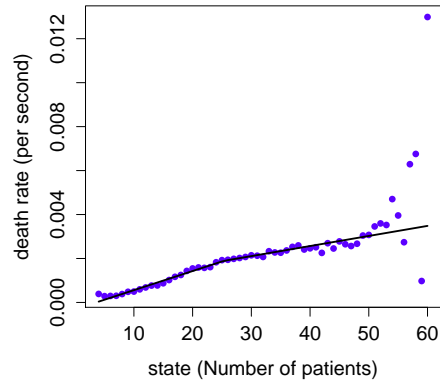
		Fitting interval	Prop. of data	Intercept (SE)	Slope (SE)	R^2	p-value
Birth rate	2 pieces linear fit	[7, 25]	52.52%	$-1.51 * 10^{-4}$ ($7.93 * 10^{-5}$)	$8.26 * 10^{-5}$ ($4.69 * 10^{-6}$)	0.948	<0.01
		[26, 37]	35.72%	$1.87 * 10^{-3}$ ($2.20 * 10^{-4}$)	$7.79 * 10^{-6}$ ($6.94 * 10^{-6}$)	0.112	0.288
	3 pieces linear fit	[7, 13]	17.38%	$4.66 * 10^{-4}$ ($8.38 * 10^{-5}$)	$2.32 * 10^{-5}$ ($8.22 * 10^{-6}$)	0.614	0.037
		[14, 25]	35.14%	$-5.92 * 10^{-4}$ ($9.10 * 10^{-5}$)	$1.05 * 10^{-4}$ ($4.59 * 10^{-6}$)	0.981	<0.01
		[26, 37]	35.72%	$1.87 * 10^{-3}$ ($2.20 * 10^{-4}$)	$7.79 * 10^{-6}$ ($6.94 * 10^{-6}$)	0.112	0.288
Death rate	2 pieces linear fit	[5, 25]	52.99%	$-3.11 * 10^{-4}$ ($4.73 * 10^{-5}$)	$8.70 * 10^{-5}$ ($2.92 * 10^{-6}$)	0.979	<0.01
		[26, 37]	35.72%	$7.32 * 10^{-4}$ ($1.73 * 10^{-4}$)	$4.59 * 10^{-5}$ ($5.47 * 10^{-6}$)	0.876	<0.01

Table 15: Piecewise linear regression results for data without time segment. (Correspond to Figure 37.)

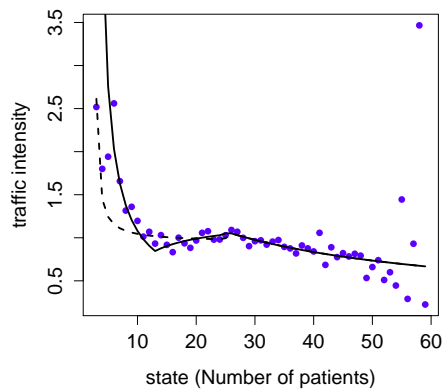
Instead of fitting a piecewise linear function to the birth-and-death rates, the bimodal structure of the empirical distribution also indicates that it may be seen as a composition of two single-mode distributions which come from 2 time periods. It leads us to divide the time of a day into 2 periods: valley



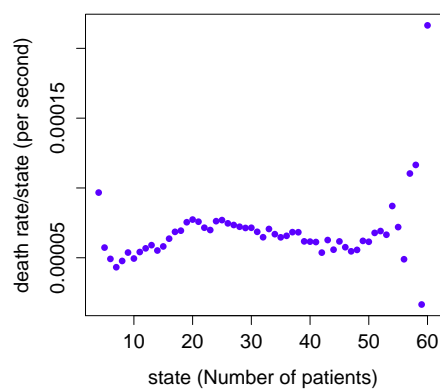
(a) Birth rates.



(b) Death rates.



(c) Traffic intensity=birth rate/death rate.



(d) Death rates per state.

Figure 37: Estimated birth and death rates without segment by time. (Use Monday to Thursday of data set 3.)

hours from 00:00 to 10:00 and peak hours from 10:00 to 00:00. We show the scaled empirical distribution of these two part in Figure 38. We can see that this time segment captures the two peaks very well.

To elaborate, for the direct fit on the left in Figure 38, the vertical black lines are the empirical distribution. The solid blue and red lines are empirical distributions for valley and peak hours. The dashed blue and red lines are

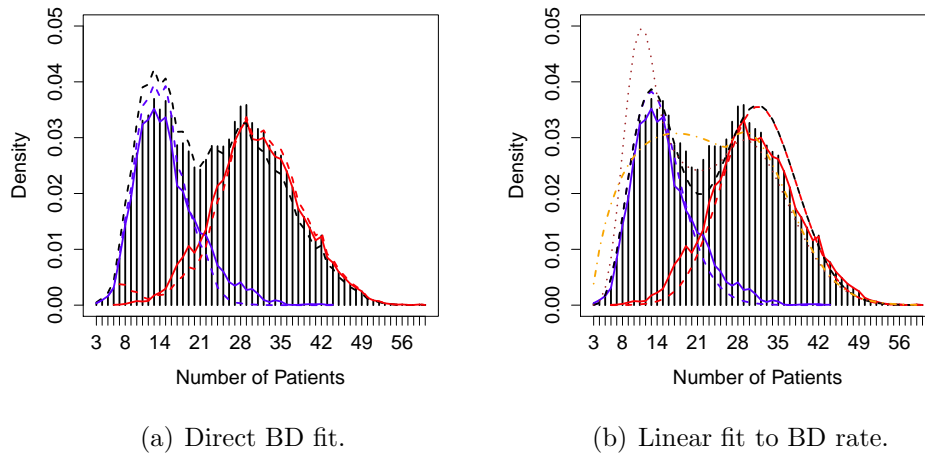
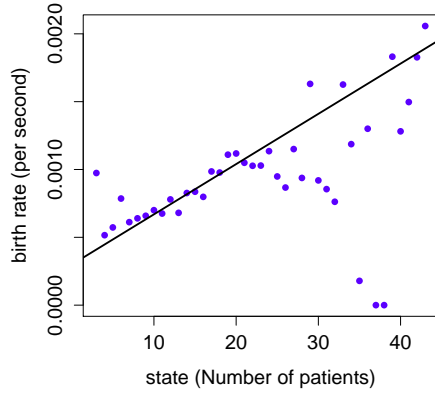


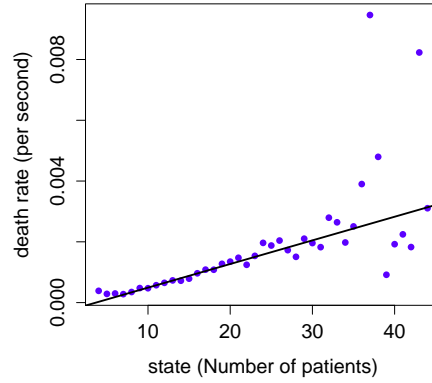
Figure 38: Time-segmented state view of the data. (Use Monday to Thursday of data set 3.)

the steady-state distributions of direct BD fitting to each part of data, while the black dashed line is the steady-state distribution of direct BD fitting to the whole data. For the linear fit to the BD rate on the right in Figure 38, the vertical black lines are the empirical distribution. The solid blue and red lines are the empirical distributions for valley and peak hours. The dashed blue and red lines are steady-state distributions of the linear fitted BD rates and the black dashed line is the sum of the dashed blue and red lines. The brown dotted line is steady distribution of the piecewise linear fitted BD rates without time segment. And the orange dot dash line is the steady distribution if we fit the birth rates by 2 piece of lines

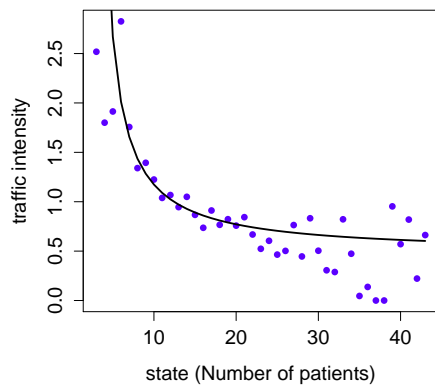
The estimated birth and death rates are shown in Figure 39 and 40. This time we see that the all the rates are approximately linear. But there are variations at the end states which are caused by having a small sample size. So we only use the state interval which corresponds to the 10% and 90% quantile points of the empirical distribution of each time periods. Specifically, for valley hours we use state interval $[9, 22]$ and for peak hours we use $[21, 40]$. Then we compute the steady-state distributions of the directly estimated BD processes and the one with linear fitted rates. The results are also shown in Figure 38 and Table 16.



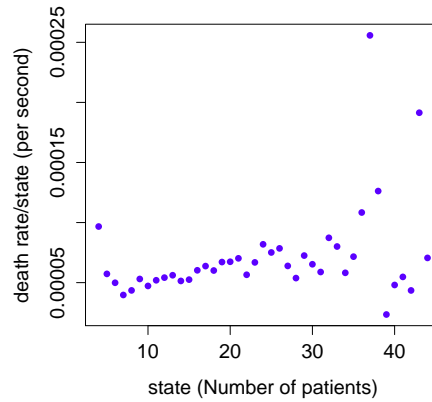
(a) Birth rates of valley hours.



(b) Death rates of valley hours.



(c) Traffic intensity=birth rate/death rate.

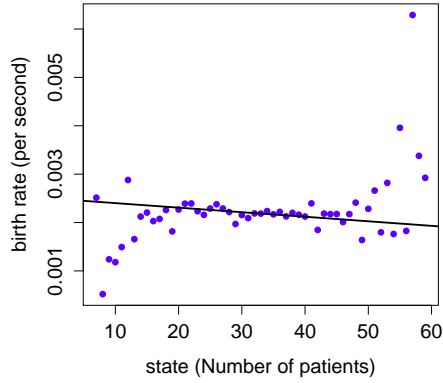


(d) Death rates per state of valley hours.

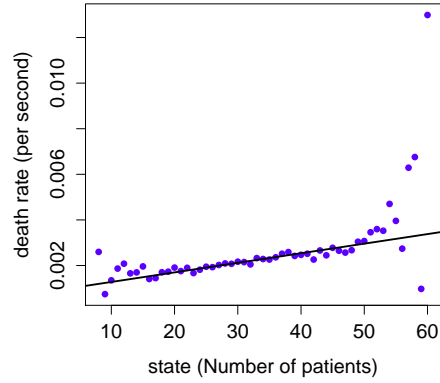
Figure 39: Estimated birth and death rates of valley hours with segment by time. (Use Monday to Thursday of data set 3.)

9. Estimating the Congestion Effect

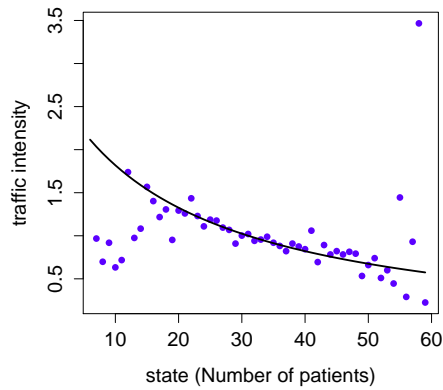
In §4 we observed that in this ED data two key effects are confounded: (i) service time (i.e., service requirement) and (ii) extra congestion (i.e., waiting, because of congestion). Of course, these notions are actually not easy (and maybe impossible) to identify, regardless of how much data we have. In any



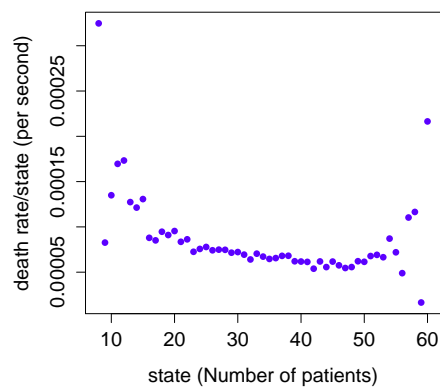
(a) Birth rates of peak hours.



(b) Death rates of peak hours.



(c) Traffic intensity=birth rate/death rate.



(d) Death rates per state of peak hours.

Figure 40: Estimated birth and death rates of peak hours with segment by time. (Use Monday to Thursday of data set 3.)

case, we do not see these separately directly from the available data.

To show the congestion effect in the ED, we look at the LOS vs number of patients seen by arrival in the ED. Figure 41 shows that this state-dependent mean of LOS is increasing as the number in the system increasing. The median is also increasing, but not so obviously.

One way to see the congestion effect is by fitting a $M_t/GI/\infty$ model

		Fitting interval	Prop. of data	Intercept (SE)	Slope (SE)	R^2	p-value
Valley hours	Birth rate	[9, 22]	36.37%	$2.99 * 10^{-4}$ ($7.00 * 10^{-5}$)	$3.70 * 10^{-5}$ ($4.37 * 10^{-6}$)	0.857	<0.01
	Death rate	[9, 22]	36.37%	$-2.85 * 10^{-4}$ ($8.96 * 10^{-5}$)	$7.78 * 10^{-5}$ ($5.60 * 10^{-6}$)	0.942	<0.01
Peak hours	Birth rate	[21, 40]	50.59%	$2.50 * 10^{-3}$ ($1.09 * 10^{-4}$)	$-9.39 * 10^{-6}$ ($3.51 * 10^{-6}$)	0.285	0.015
	Death rate	[21, 40]	50.59%	$8.58 * 10^{-4}$ ($9.94 * 10^{-5}$)	$4.20 * 10^{-5}$ ($3.20 * 10^{-6}$)	0.905	<0.01

Table 16: Piecewise linear regression results for data with time segment. (Correspond to Figure 39 and 40.)

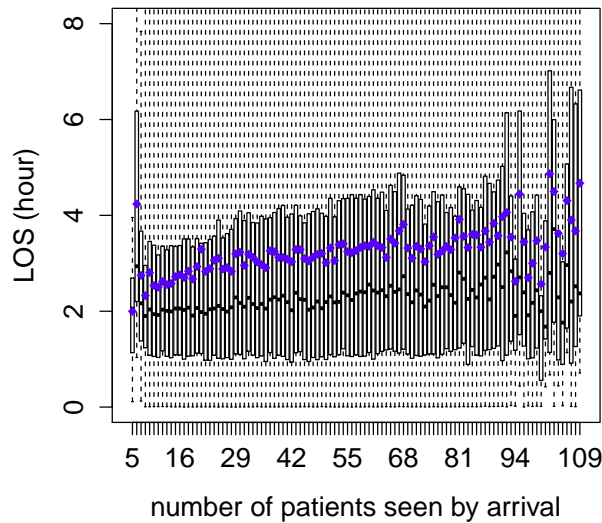


Figure 41: Number of patients seen by arrival vs LOS for ED.

where the length of stay distribution is estimated by taking the maximum of the cumulative distribution functions of 24 empirical distributions of length of stay of each hour. In other words, we regard the cumulative distribution function got by taking maximum as the true service rate. The departure rate and number in the system predicted by the model is shown in Figure

42. The difference between the true and predicted occupancy level can be seen as the degree of congestion. However, the drawback of this method is that even without congestion, the service rate of the ED is time-varying due to staffing, etc. Even though we are convinced that there exists congestion, to quantify and assess the congestion effect is still a hard problem.

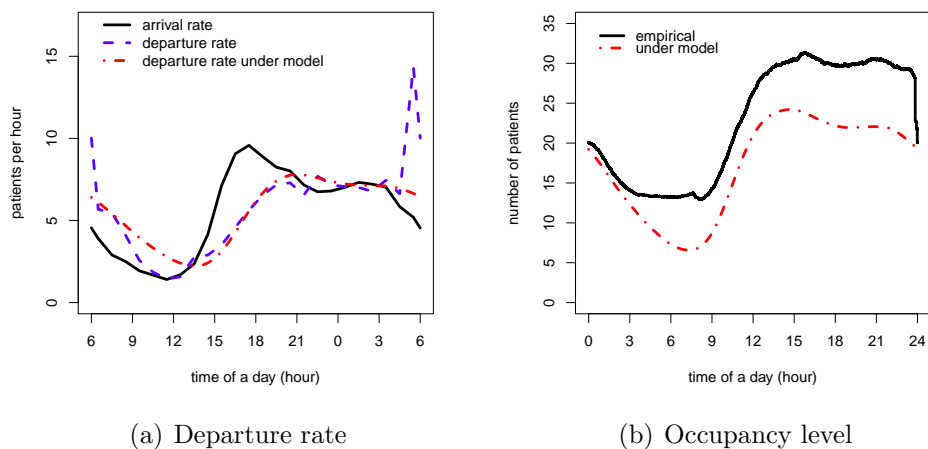


Figure 42: $M_t/GI/\infty$ model using the maximum CCDF.

Acknowledgement. We thank Avishai Mandelbaum, Galit Yom-Tov and their colleagues at the Technion IE&M Laboratory for Service Enterprise Engineering (SEELab) for providing access to the Israeli Rambam hospital data. We thank NSF for research support through CMMI 1265070.

- [1] W. Whitt, X. Zhang, A data-driven model of an emergency department, Columbia University, <http://www.columbia.edu/~ww2040/allpapers.html> (2016).
- [2] D. Bertsimas, G. Mourtzinou, Transient laws of nonstationary queueing systems and their applications, *Queueing Systems* 25 (1997) 315–359.
- [3] B. H. Fralix, G. Riano, A new look at transient versions of Little’s law, *Journal of Applied Probability* 47 (2010) 459–473.
- [4] S. Kim, W. Whitt, Estimating waiting times with the time-varying little’s law, *Probability in the Engineering and Informational Sciences* 27 (04) (2013) 471–506.
- [5] W. Whitt, X. Zhang, Data analysis and the time-varying little’s law, in preparation, Columbia University, <http://www.columbia.edu/~ww2040/allpapers.html> (2016).
- [6] J. Dong, W. Whitt, Stochastic grey-box modeling of queueing systems: fitting birth-and-death processes to data, *Queueing Systems* 79 (2015) 391–426.
- [7] J. Dong, W. Whitt, Using a birth-and-death process to estimate the steady-state distribution of a periodic queue, *Naval Research Logistics* 62 (8) (2015) 664–685.
- [8] W. Whitt, Fitting birth-and-death queueing models to data, *Statistics and Probability Letters* 82 (2012) 998–1004.
- [9] S. Kim, W. Whitt, Choosing arrival process models for service systems: Tests of a nonhomogeneous Poisson process, *Naval Research Logistics* 17 (2014) 307–318.
- [10] S. Kim, W. Whitt, Are call center and hospital arrivals well modeled by nonhomogeneous Poisson processes?, *Manufacturing and Service Oper. Management* 16 (3) (2014) 464–480.

- [11] M. H. Kutner, C. Nachtsheim, J. Neter, Applied linear regression models, 4th Edition, McGraw-Hill/Irwin, 2004.
- [12] P. J. Brockwell, R. A. Davis, Introduction to Time Series and Forecasting, Springer Science & Business Media, 2006.
- [13] D. J. Daley, D. Vere-Jones, An Introduction to the Theory of Point Processes, 2nd Edition, Vol. II, Springer, Oxford, U. K., 2008.
- [14] M. Armony, S. Israelit, A. Mandelbaum, Y. Marmor, Y. Tseytlin, G. Yom-Tov, Patient flow in hospitals: a data-based queueing-science perspective, *Stochastic Systems* 5 (1) (2015) 146–194.
- [15] S. Maman, Uncertainty in the demand for service: The case of call centers and emergency departments, Master’s thesis, Technion-Israel Institute of Technology (2009).
- [16] D. R. Cox, P. A. W. Lewis, The Statistical Analysis of Series of Events, Methuen, London, 1966.
- [17] K. W. Fendick, W. Whitt, Measurements and approximations to describe the offered traffic and predict the average workload in a single-server queue, *Proceedings of the IEEE* 71 (1) (1989) 171–194.
- [18] P. Billingsley, Statistical Inference for Markov Processes, University of Chicago press, Chicago, 1961.
- [19] N. Keiding, Maximum likelihood estimation in the birth-and-death process, *Ann. Statist.* 3 (1975) 363–372.
- [20] R. W. Wolff, Problems for statistical inference for birth and death queueing models, *Operations Research* 13 (1965) 343–357.
- [21] M. El-Taha, S. Stidham, Sample-Path Analysis of Queueing Systems, Kluwer, Boston, 1999.